# Characterization of retinal guanylate cyclase-activating protein 3 (GCAP3) from zebrafish to man

Yoshikazu Imanishi,[1] Ning Li,[4,*] Izabela Sokal,[1] Mathew E. Sowa,[5,6,7] Olivier Lichtarge,[6,7,8,9,10] Theodore G. Wensel,[5,6,7] David A. Saperstein,[1] Wolfgang Baehr[4] and Krzysztof Palczewski[1,2,3]

[1]Department of Ophthalmology, [2]Pharmacology, and [3]Chemistry, University of Washington, Seattle, WA 98195, USA
[4]Department of Ophthalmology, Moran Eye Center, University of Utah Health Science Center, Salt Lake City, Utah 84112–5330, USA
[5]Verna and Marrs McLean Department of Biochemistry and Molecular Biology, [6]Program in Structural and Computational Biology and Molecular Biophysics, [7]W.M. Keck Center for Computational Biology, [8]Department of Molecular and Human Genetics, [9]Program in Developmental Biology, [10]Human Genome Sequencing Center, Baylor College of Medicine, Houston, Texas 77030, USA

## Abstract

Calmodulin-like neuronal $Ca^{2+}$-binding proteins (NCBPs) are expressed primarily in neurons and contain a combination of four functional and nonfunctional EF-hand $Ca^{2+}$-binding motifs. The guanylate cyclase-activating proteins 1–3 (GCAP1–3), the best characterized subgroup of NCBPs, function in the regulation of transmembrane guanylate cyclases 1–2 (GC1–2). The pairing of GCAPs and GCs *in vivo* depends on cell expression. Therefore, we investigated the expression of these genes in retina using *in situ* hybridization and immunocytochemistry. Our results demonstrate that *GCAP1, GCAP2, GC1 and GC2* are expressed in human rod and cone photoreceptors, while *GCAP3* is expressed exclusively in cones. As a consequence of extensive modification, the *GCAP3* gene is not expressed in mouse retina. However, this lack of evolutionary conservation appears to be restricted to only some species as we cloned all three *GCAP*s from teleost (zebrafish) retina and localized them to rod cells, short single cones (*GCAP1–2*), and all subtypes of cones (*GCAP3*). Furthermore, sequence comparisons and evolutionary trace analysis coupled with functional testing of the different GCAPs allowed us to identify the key conserved residues that are critical for GCAP structure and function, and to define class-specific residues for the NCBP subfamilies.

## Introduction

$Ca^{2+}$-binding proteins from the calmodulin (CaM) superfamily, termed GCAPs, are involved in the regulation of photoreceptor GC (Polans *et al*., 1996). GCAPs stimulate GC1 and/or GC2 in low $[Ca^{2+}]_{free}$, and this regulation is responsible, in part, for modulating the sensitivity of photoreceptor cells and extending their operation through a broad range of light intensities (Mendez *et al*., 2001). Two proteins, GCAP1 and GCAP2, which share only ≈50% homology were discovered initially (reviewed in Polans *et al*., 1996). More recently, we reported the presence of a new retina-specific GCAP, termed GCAP3 (Haeseleer *et al*., 1999), and GCIP (Li *et al*., 1998). For detailed understanding of phototransduction, the pairing of GCAPs with GCs is of great importance, however, it remains unclear. *In situ* hybridization with short *GCAP1* RNA probes showed the transcript abundantly present in cone myoid regions and, to a lesser degree, in rod inner segments in human and bovine retina (Palczewski *et al*., 1994; Subbaraya *et al*., 1994). The intensity of GCAP1's

immunoreactivity was strong in cone outer segments for all mammalian species tested but weaker in rod outer segments (ROS) (Gorczyca *et al*., 1995), particularly in primates (Kachi *et al*., 1999), cats (Cuenca *et al*., 1998), and mouse retina (Cuenca *et al*., 1998; Howes *et al*, 1998).

Initially, GCAP2 was localized in rod photoreceptors (Dizhoor *et al*, 1995). However, in subsequent experiments, we and colleagues localized GCAP2 to the cone inner segments, somata, and synaptic terminals and, less significantly, to the rod inner segments and inner retinal neurons. A number of interesting differences were observed between species (Otto-Bruc *et al*., 1997; Cuenca *et al*., 1998; Kachi *et al*., 1999). In mouse retina, GCAP2 was nearly undetectable in cones (Howes *et al*., 1998). All of these studies were carried out initially without knowledge of the existence of GCAP3 (Haeseleer et al., 1999), whose expression pattern and localization had not yet been reported.

Mammalian photoreceptors express two retina-specific membrane-associated types of GCs. GC1 immunoreactivity in human retina was detected in the photoreceptor outer segments, primarily in cones (Dizhoor *et al*, 1994; Liu *et al*., 1994). Although radioisotopic *in situ* hybridization localized human *GC2* mRNA to photoreceptor inner segments and outer nuclear layer (Lowe *et al*., 1995), a higher resolution technique is required to determine the expression in rods and cones. Electron microscopy of rat retina showed that both

*Correspondence*: Dr Krzysztof Palczewski, [1]Department of Ophthalmology or Dr Wolfgang Baehr, [4]Department of Ophthalmology, as above.
E-mail: palczews@u.washington.edu

*Present address*: Novasite Pharmaceuticals, Inc., 3520 Dunhill Street, San Diego, CA 92121, USA

cyclases are located in the rods (Yang & Garbers, 1997). However, because of the low abundance of cones in rat retina, localization of GCs to cones was not characterized.

The identification of a number of $Ca^{2+}$-binding proteins that interact with multiple GCs suggests a complex regulation of photoreceptor GCs. Therefore, in this study we investigated the expression of GCAPs and GCs in vertebrate retinas using nonisotopic *in situ* hybridization supported by immunocytochemical techniques. Using evolutionary trace analysis (ET), we also identified the key conserved residues that are critical for GCAP structure and function, and we defined class-specific residues for the NCBP subfamilies.

## Materials and methods

### SDS-PAGE and immunoblotting

SDS-PAGE was performed using 12.5% polyacrylamide gels (Laemmli, 1970). The protein electrotransfer onto immobilon-P (Millipore, Bedford, Massachusetts, USA) was carried out with a Hoeffer mini-gel system (Amersham Pharmacia Biotech. Piscataway, New Jersey, USA). For immunoblotting, the membrane was blocked with 3% BSA in phosphate-buffered saline (PBST; 136 mM NaCl, 11.4 mM sodium phosphate, 0.1% Triton X-100, pH 7.4) and incubated for 1.5 h with anti-GCAP3-antibody at a dilution of 1 : 2000. A secondary antibody conjugated with alkaline-phosphatase (Promega, Madison, Wisconsin, USA) was used at a dilution of 1 : 5000. Antibody binding was detected by incubation with NBT/BCIP (Promega, Madison, Wisconsin, USA).

### Cloning of zebrafish GCAP1, GCAP2 and GCAP3 cDNAs

Based on the expressed sequence tag clones (e.g. BG307360, BG305035, BG305375 deposited by Stephen L. Johnson, Washington University School of Medicine), zebrafish *GCAP1* coding region was amplified from a λZAPII zebrafish retina cDNA library (gift of Dr David Hyde, Notre Dame) with sense primer ZG1-S (5′-ATGGGCAATTCAACGGGC), antisense primer ZG1-A (5′-CGAGCCCCTGCTACAAACTC) using standard PCR conditions with Taq polymerase. The 5′-untranslated region of *GCAP1* was amplified with ZG1-A and universal primer T3. The 3′-untranslated region of *GCAP1* was amplified with ZG1-S and T7. *GCAP2* and *GCAP3* were amplified using similar approaches. The specific primers are ZG2-S (5′-ATGGGTCAGCGGCTCAGC) and ZG2-A (5′–GCCATGGGCGCCAAGGCATCC) for amplifying *GCAP2*; ZG3-A (5′–ACGTGTGTGAGGTCCATC) and ZG3-S (5′–GCCAT-GGGCGCCAAGGCATCC) for amplifying *GCAP3*. cDNA fragments of *GCAP*s were cloned into PCRII-TOPO vector (Invitrogen, Carlsbad, California, USA).

### Identification of mouse GCAP3 gene

Based on the sequence fragments (Accession numbers: 544850, 13770026, 20684911, 14011120) found from the mouse trace archives database (http://www.ncbi.nlm.nih.gov/blast/mmtrace.html), the mouse *GCAP3* genomic fragment, including exon 1, was amplified from mouse genomic DNA with sense primer mG3–1S (5′–ACCACACATTCAAATACATGAGTC) and antisense primer mG3–1 A (5′-GACGTGAGTTACAAATCAAGTTG) using standard PCR conditions with the Expand™ High Fidelity PCR System (Roche Molecular Biochemicals, Indianapolis, Indiana, USA). DNA fragments of m*GCAP3* genes were cloned into PCRII-TOPO vector (Invitrogen, Carlsbad, California, USA) and sequenced. Additional mouse genomic fragment including partial *GCAP3* exon 3 and intron C, was amplified with sense primer mG2-3S (5′-GTTGAATG-

TATTCTTGGGTACT) and antisense primer mG3-3 A (5′-GTC-TATGTCAATATTATGAAGC) based on trace files (ml2C-c274f04.p1ca and ml2C-c274f04.p1c from http://trace.ensembl.org/ and deposited by the Sanger Centre).

### Tissue preparation for immunocytochemistry and in situ hybridization

The zebra fish were anesthetized with 0.02% methane tricaine sulfate, as approved by the Animal Care Committee at the University of Washington, and killed. Anterior segments of zebrafish eyes were removed and then eyecups were fixed for 4 h in 4% paraformaldehyde in 0.1% phosphate buffer (PB; 100 mM sodium phosphate, pH 7.4). A human eyecup was fixed at 4 h postmortem in 4% paraformaldehyde for 12 h. Retinal tissues were infiltrated with 20% sucrose in PB, and then embedded in 33% OCT compound (Sakura, Tokyo, Japan) diluted with 20% sucrose in PB. Zebrafish and human retinas were sectioned at 5 µm and 12 µm, respectively.

### Immunocytochemistry

Human GCAP3 (hGCAP3) was expressed and purified as described previously (Haeseleer *et al.*, 1999). Purified hGCAP3 was used to immunize a mouse to obtain an anti-GCAP3 antiserum. To block nonspecific labelling, human retinal sections were incubated in 1.5% normal goat serum in PBST for 15 min at room temperature. Sections were incubated overnight at 4 °C in purified anti-GCAP3 polyclonal antibodies in PBST. Controls were prepared by absorbing the anti-GCAP3 antibodies with an excess amount of GCAP3 (1 µg/mL) or GCAP1/2 (2 µg/mL). Sections were rinsed in PBST and incubated with indocarbocyanine (Cy3)-conjugated goat anti-mouse IgG. Then, sections were rinsed in PBST, mounted in 50 µL 2% 1,4-diazabicyclo-2,2,2-octane in 90% glycerol to retard photobleaching. Sections were analyzed under an episcopic-fluorescent microscope (Nikon, Melville, New York, USA). Digital images were captured with a digital camera (Diagnostic Instruments; Sterling Heights, MI).

### In situ hybridization

cDNA fragments of *GCAP*s and *GC*s were cloned into PCRII-TOPO vector or pGEM-3Zf(+) plasmid vectors, and linearized with appropriate endonucleases. Antisense and sense RNA probes (500–700 bases in length for *GCAP*s and *GC2*, 1.6 kb for *GC1*) were synthesized by run-off transcription from the SP6 or T7 promoter with digoxigenin-UTP, as recommended in the manufacture's protocol (Roche Molecular Biochemicals, Indianapolis, Indiana, USA). *In situ* hybridization technique of retinal sections are as described previously (Barthel & Raymond, 2000), with modifications. Sections stored at –80 °C were thawed, rehydrated, and fixed in 4% paraformaldehyde for 30 min. After fixation, sections were washed three times in phosphate-buffered saline (PBS) and then digested with proteinase K (5 µg/mL) for 10–15 min. After digestion, sections were fixed in 4% paraformaldehyde for 30 min, washed three times in PBS and treated with 0.25% acetic anhydride in 0.1 M triethanolamine. After washing with 1 × SSC, sections were hybridized at 65 °C for 16 h with 0.1 µg/mL RNA probes in the hybridization solution (Rosen & Beddington, 1994). After hybridization, the slides were washed in 1 × SSC at room temperature for 0.5 h, then in 50% formamide in 2 × SSC at 65 °C for 2 h, and then treated with RNAse A (5 µg/mL) at 37 °C for 1 h to digest unbound probe. To eliminate the endogenous alkaline phosphatase (AP) activity, sections were treated with 20 mM HCl for 5 min, and then blocked with 0.5% blocking solution (Roche Molecular Biochemicals, Indianapolis, Indiana, USA) in Tris-buffered saline with 0.1% Tween 20 (TBST; 25 mM Tris, 137 mM NaCl, 3 mM KCl, and 0.1% Tween 20) at room

temperature for 0.5 h. Sections were incubated at 4 °C for 16 h with anti-digoxigenin antibodies conjugated with AP. Hybridization signal was detected by incubation with NBT–BCIP (Promega, Madison, Wisconsin, USA) for 4–48 h at room temperature. Sections were rinsed with dH$_2$O. For double labelling, after colouring reactions sections were incubated with 1.5% normal goat serum in PBST for 15 min at room temperature and then incubated with antibodies to human red/green opsin (generated against N-terminal peptide in human red/green cone opsin; a gift from J. Saari, University of Washington) or human blue cone opsin (JH455 serum, specific for the C-terminus of human blue opsin; a gift from Jeremy Nathans, Johns Hopkins University School of Medicine). Sections were then rinsed in PBST and incubated with indocarbocyanine (Cy3)-conjugated goat anti-rabbit IgG. Sections were rinsed in PBS, mounted in 50 μL 2% 1,4-diazabicyclo-2,2,2-octane in 90% glycerol to retard photobleaching. Sections were analyzed under fluorescent microscope. Fluorescent images and transparent images were imported into Adobe Photoshop 5.0 and merged images were generated.

### RNA dot blots

Unlabelled sense transcripts were generated from cloned cDNAs following the manufacturer's specifications. Sense transcripts, 0.1 ng, 1 ng and 10 ng were blotted onto Hybond NX membrane (Amersham Pharmacia Biotech. Piscataway, New Jersey, USA) and bound by cross-linking. High stringency hybridization was carried out at 65 °C for 16 h in the hybridization solution. Digoxygenin-labelled cRNA probes were diluted to 100 ng/mL. All procedures for post-hybridization and detection were as described for *in situ* hybridization.

### Expression of GCAP3 *and GC assay*

The entire coding region of *zGCAP3* was cloned into pET28a (Novagen, Madison, Wisconsin, USA), and expressed in Bl21(DE3)LysS strain. Bacterially expressed GCAP3-His6 was purified using Ni-NTA agarose (Qiagen, Valencia, California, USA). The GC assay was performed using [α-$^{32}$P] GTP and washed ROS (Gorczyca *et al*., 1995). Ca$^{2+}$ was calculated using the Chelator 1.00 (Schoenmakers *et al*., 1992) and adjusted in Ca$^{2+}$ titration experiments to a higher concentration by increasing the amount of CaCl$_2$.

### Calculation of the phylogenetic tree

A phylogenetic tree was constructed from the aligned sequences using the ClustalW program. Evolutionary distances of the sequences (k) were estimated using the proportion of different amino acids between the two sequences (p), with correction for multiple substitutions of k = –ln(1 – p – 0.2 p2) (Kimura, 1991) by Protdist of PHYLIP (version 3.573). The phylogenetic tree was constructed by the neighbour-joining method using the Neighbour program of PHYLIP (version 3.573). Bootstrap resamplings were performed by Seqboot program of PHYLIP (version 3.573).

### Evolutionary trace analysis of NCBP and GCAP families

Evolutionary trace analysis (ET) was performed as previously described (Lichtarge *et al*., 1996; Sowa *et al*., 2001). Briefly, ET uses the sequence identity tree (dendrogram) produced from the multiple sequence alignment (MSA) of a protein family to divide the family into subgroups based on evolutionary relatedness. The number of subgroups can be varied and referred to as the rank of the trace. Residue positions that have an identical residue within each of the subgroups, but whose identity varies among the subgroups, are termed class-specific. These class-specific residues are considered to

be important for delineating the functional specificities of the different subgroups and can provide information for designing targeted mutagenesis experiments for separation of function (Sowa *et al*., 2001). The amino-acid sequence of bovine GCAP2 was used in a BLAST search to retrieve similar sequences. Redundant and partial sequences were removed from the BLAST output and the remaining 106 unique sequences were aligned using the Genetic Computer Group (GCG, Wisconsin, USA) program PILEUP with the default matrix. The 33 members of the GCAP subfamily were extracted from this MSA, realigned, and the resulting MSA was used as the input for the ET of the GCAP family. The results were mapped onto the structure of Ca$^{2+}$-bound bovine GCAP2. Rank 5 was chosen for the final analysis because this choice partitioned the dendrogram into individual GCAP subfamilies and GCIP. For the ET of the entire NCBP family, the initial MSA was used, including the GCAP family. Rank 30 was chosen for the analysis as above this rank, random signals begin to dominate the output At this rank, the major subgroups are GCAP1, GCAP2, GCAP3, GCIP, calsenilin, recoverin, visinin, neurocalcin, and frequenin, with additional groups formed either by single sequences associated with each of these groups or divisions within these groups.

## Results

### In situ *localization of* GCAP3 *mRNA in human retina*

The distribution of human GCAPs (hGCAPs) was investigated by nonisotopic *in situ* hybridization. The digoxigenin-conjugated *GCAP3* antisense RNA probe hybridized only to the cells proximal to outer limiting membrane, and the signals were observed only in cone inner segments and cell bodies (Fig. 1A, left). *GCAP3* sense RNA probe control did not produce a hybridization signal (Fig. 1A, right). For GCAP1 and GCAP2, the hybridization signal employing antisense RNA probe was observed throughout the outer nuclear layer (Fig. 1B and C left, respectively) with the most intense labelling observed in the cone inner segment and cell bodies. For GCAP2, weak signals were observed in a subpopulation of inner nuclear neurons and ganglion cells.

RNA dot blots were employed to test the specificity of RNA–RNA hybridization. Unlabelled sense transcript of *GCAP*s were blotted onto hybond NX membrane and hybridized under the identical condition as *in situ* hybridization, using GCAP antisense probes. Each GCAP antisense probe hybridized specifically to the corresponding GCAP sense probe (Fig. 1D). These results indicate that the hybridization conditions employed here are GCAP subclass specific.

To specify the subtype of GCAP3-positive cones, sections were double stained by *in situ* hybridization with the GCAP3 antisense probe and immunocytochemistry, using anti-blue and anti-red/green cone opsins. *GCAP3* mRNA is expressed in cones that are immunoreactive with anti-blue (Fig. 2A) and anti-red/green opsin (Fig. 2B), whereas GCAP1 and GCAP2 are present in both rods and cones.

### Subcellular localization of GCAP3

To investigate the specificity of the anti-GCAP3 antiserum, reactivity of GCAP1/GCAP2/GCAP3 was tested by immunoblotting. Anti-GCAP3 antiserum recognized recombinant hGCAP3 (Fig. 3A). Immunofluorescence microscopy of human retina revealed that GCAP3 was present in a limited number of photoreceptor outer segments (Fig. 3B). By morphological criteria, hGCAP3 appears to be present in cone outer segments and not ROS (Fig. 3C). Importantly, this result is consistent with the *in situ* hybridization
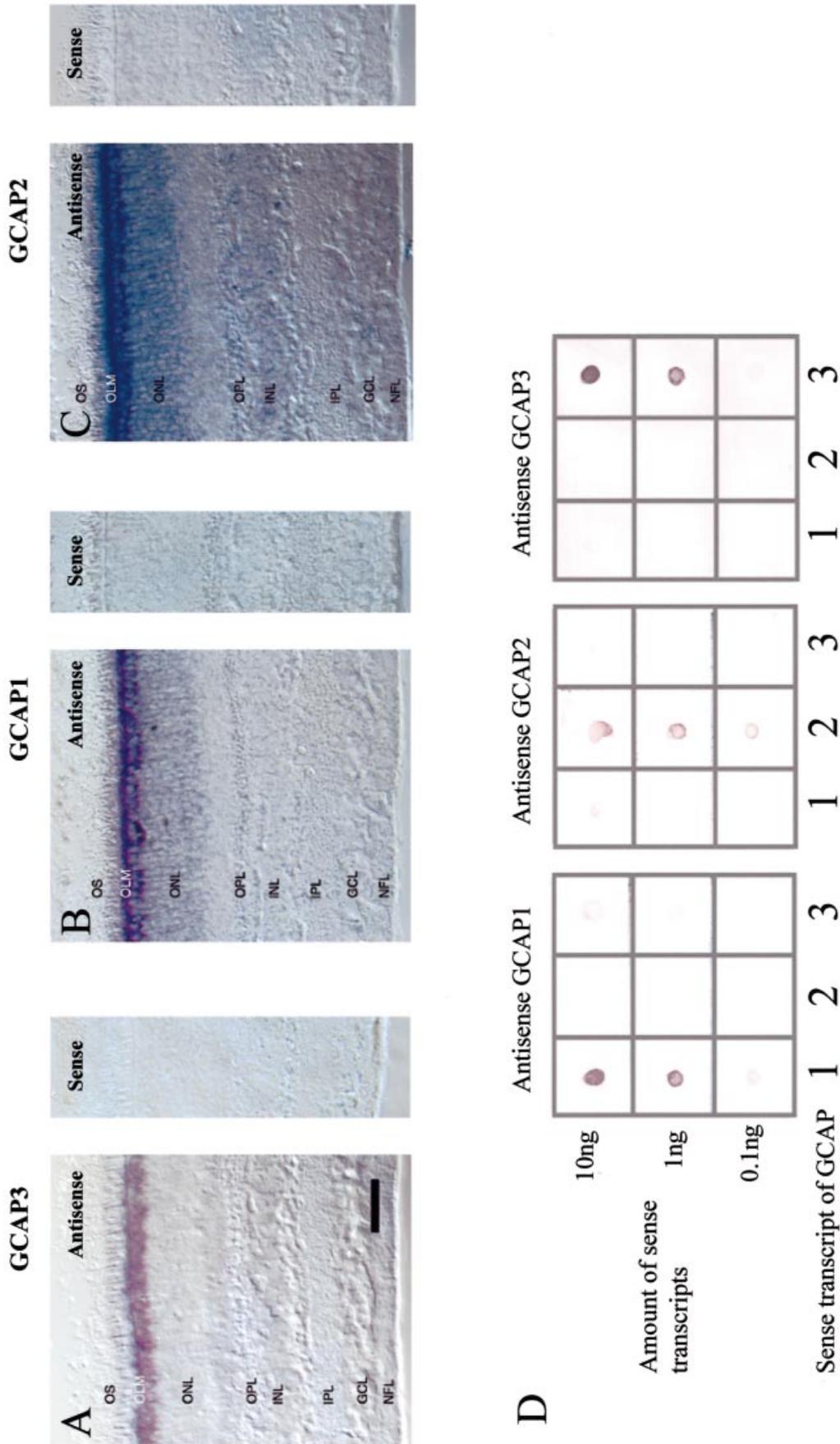
FIG. 1. *In situ* hybridization of human GCAPs and specificity of hybridization. (A) *In situ* hybridization of GCAP3 transcripts using antisense (left) and sense (right) RNA. The strong signal is in cone inner segment and cell bodies. No signal is observed in rod photoreceptors. Bar, 50 μm (A–C). (B) *In situ* hybridization of GCAP1 transcripts using antisense (left) and sense (right) RNA. The strongest signal is in cone inner segment and cell bodies. Rod inner segments and cell bodies are also labelled. (C) *In situ* hybridization of GCAP2 transcripts using antisense (left) and sense (right) RNA. The strongest signal is in cone inner segment and cell bodies. Rod inner segments, cell bodies and inner retinal neurons are also labelled. (D) RNA dot blots of human GCAP transcripts. Different amounts of GCAP sense transcripts (10, 1, and 0.1 ng) were blotted on Hybond-NX membrane. GCAP1 cRNA probe hybridized specifically to GCAP1 sense RNA blotted on left column (left). GCAP2 hybridized to GCAP2 sense transcripts blotted on middle column. GCAP3 antisense probe hybridized to GCAP3 sense transcripts blotted on right column. Abbreviations: OS, photoreceptor outer segments; IS, photoreceptor inner segments; ONL, outer nuclear layer; OPL, outer plexiform layer; INL, inner nuclear layer; IPL, inner plexiform layer; GCL, ganglion cell layer; and NFL, nerve-fibre layer.
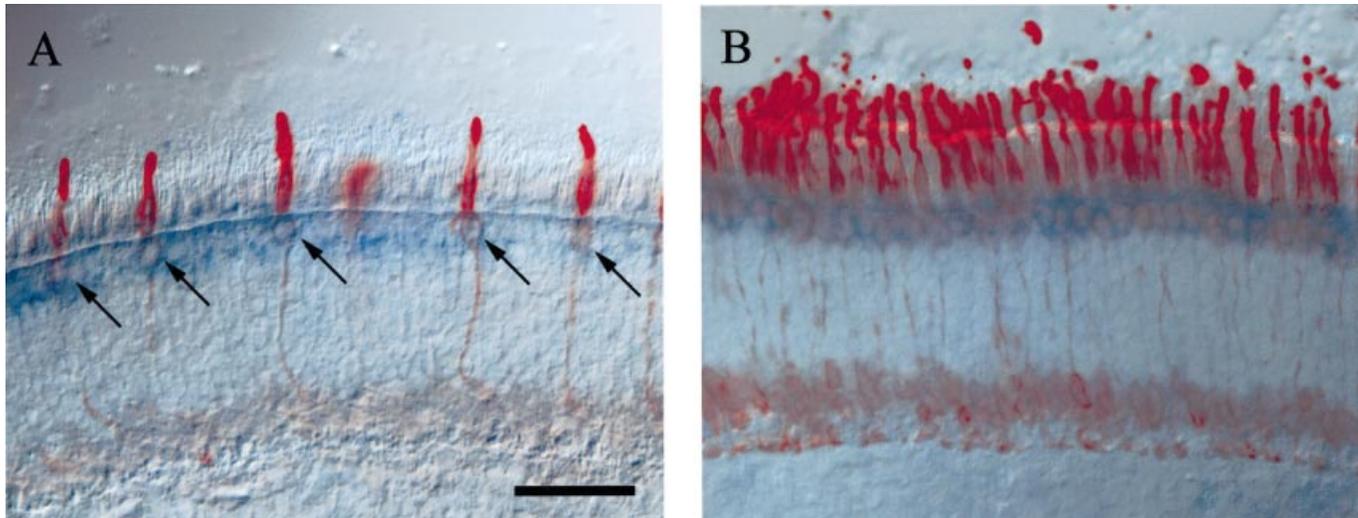
FIG. 2. Double labelling with DIG labelled GCAP3 cRNA (blue) with anti-cone opsins antibodies (red). (A) Double labelling with anti-blue cone opsin. Anti-blue cone opsin labels cone photoreceptors which hybridizes GCAP3 cRNA probe (blue). (B) Double labelling with anti-red/green cone opsin. Red/green cones are labelled with GCAP3 cRNA. Scale bar, 50 μm

results. The immunolabelling was abolished by preincubation with hGCAP3 (Fig. 3D), but was not altered by incubation with hGCAP1/hGCAP2 (Fig. 3E).

*Localization of GCs in human retina*

*In situ* hybridization was used to determine the cell type specific expression pattern of photoreceptor GCs. cDNA, corresponding to the low-homology intracellular domain (≈1.6 kb in length), was used as a template for the probe. GC1 signals (purple) were strongest in the cone inner segments and were also intense in the rod inner segments and cell bodies (Fig. 4A, left). Weak signals were observed in the inner nuclear and ganglion cell layers (Fig. 4A, left) and no signal was observed for the sense probe (Fig. 4A, right). This localization of GC1 result is consistent with previous immunocytochemical reports (Dizhoor *et al*., 1994; Liu *et al*., 1994). Isotopic *in situ* hybridization showed exclusive expression of *GC1* mRNA in the photoreceptor layer of monkey retina (Shyjan *et al*., 1992), yet as a consequence of low resolution and high background of this method, precise localization of the photoreceptor cell-type was not possible. To determine *GC1* cell-specific expression, an immunohistochemical/*in situ* hybridization double staining technique with cone-specific antibodies was employed. Double staining with anti-blue opsin antibodies (red signal) shows that *GC1* is expressed in blue cones (Fig. 4B). Double labelling with anti-red/green opsin antibodies (red signal) shows that *GC1* is expressed in red/green cones (Fig. 4C). These results indicate that *GC1* is expressed in all classes of cones.

Using a similar method, *in situ* hybridization of *GC2* was carried out using cDNA corresponding to the extracellular domain (≈0.7 kb in length) to produce sense and antisense RNA probes. The digoxigenin labelled antisense *GC2* probe showed intense labelling in cone photoreceptors, and weak labelling in rod photoreceptors (Fig. 5A). *GC2* is expressed in blue cones (Fig. 5B) and red/green cones (Fig. 5C), as shown by labelling using *in situ* hybridization and immunocytochemistry. A weaker signal was observed for *GC2*, compared to *GC1*, indicating that *GC1* may be expressed at higher levels than *GC2*. These results

suggest that *GC1* and *GC2* are coexpressed in all cones and rods in human retina.

*Identification of mouse* GCAP3 *genomic sequence*

Several genomic fragments with homology to the human *GCAP3* genomic sequence were found by searching the mouse trace database using megablast search program (http://www.ncbi.nlm.nih.gov/blast/mmtrace.hrml). Primers were designed based on these mouse traces (544850, 13770026, 20684911, 14011120, ml2C-c274f04.p1ca and ml2C-c274f04.p1c) and used to amplify mouse *GCAP3* genomic DNA using mouse genomic DNA as a template. Two separate DNA fragments that are homologous to human *GCAP3* gene were amplified. These genomic fragments consist of 838 and 308 base pairs, respectively. The BlastN program was utilized to compare these sequences with the human *GCAP3* genomic sequence (accession numbers: AC016948, AF109998, and AF110000). Human and mouse *GCAP3* genomic sequences around exon 1 were aligned (Fig. 6A). This region showed 67% nucleotide identity. Exon 1, especially, having the greatest homology (72%). In mouse, exon 1 of *GCAP3* contains several deletions that create three frame shifts. Functional exon–intron junction sites were not found. Figure 6B shows the comparison of intron A sequences downstream of exon 1. This region shows even higher homology (83% 279/334 nucleotides) than exon 1. The comparison of partial intron C and exon 3 sequences (Fig. 6C) reveals high identity (69% 196/282 nucleotides) in this region of the gene and even higher identity in the exon 3 area (75% 61/81 nucleotides). These results indicate that these mouse genomic sequences are highly homologous to the human *GCAP3* gene. We were unable to identify other genomic sequences closely related to human *GCAP3* exon 1 and exon 3 in the mouse.

Mouse exon 1 and partial exon 3 sequences were conceptually translated and aligned with the amino-acid sequence of human GCAP3. Translated exon 1 sequences showed low identity (46% 32/69 amino acids) despite high identity at the nucleotide level. The translated mouse exon 1 sequence does not show a potential myristoylation site or functional EF-hands, and has three stop codons and three frame shifts (Fig. 6D, arrows). Translated mouse exon 3 exhibits high identity (63% 17/27 amino acids) with human GCAP3
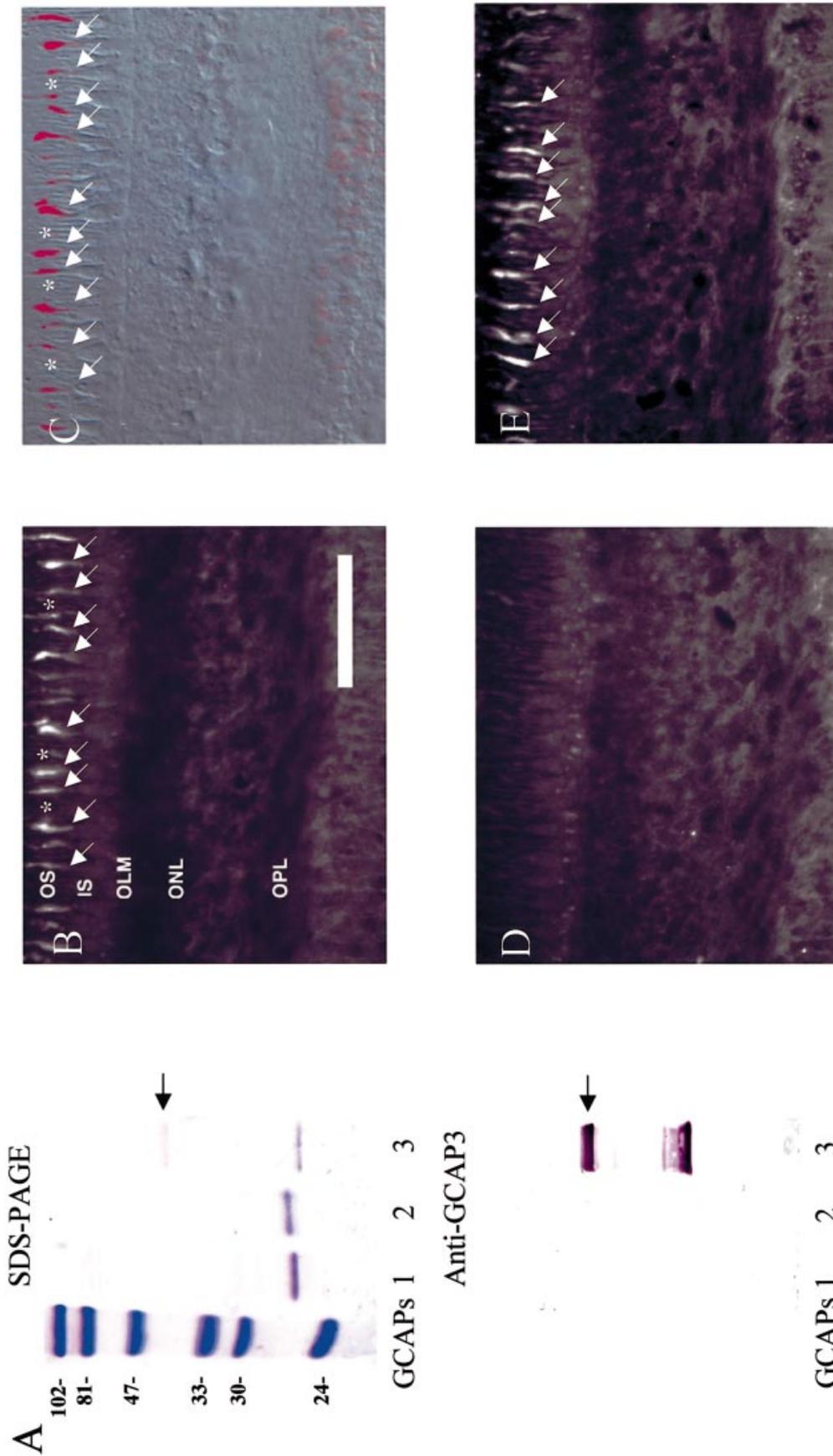
Fig. 3. Immunolocalization of GCAP3 in human retina. (A) Specificity of anti-GCAP3 antibodies. Lane 1, purified GCAP1 (0.1 µg); lane 2 purified GCAP2 (0.1 µg); lane 3 purified GCAP3 (0.1 µg). Top, SDS-polyacrylamide gel stained with Coomassie Brilliant Blue R-250. Bottom, reactivity of anti-GCAP3 analyzed by Western blotting. The arrows indicate dimeric forms of GCAP3 seen in SDS-PAGE and on immunoblotting. The dimeric form of GCAP3 was confirmed using separate immunoblot and a generic antibody, G2, which recognizes all GCAPs. (B–D) Immunofluorescence localization of GCAP3 in human retina. (B) GCAP3 immunolabelling is specific to cone outer segments. (C) Fluorescent image from B was merged with a transparent image captured by Nomarski/DIC optics. (D) Addition of purified GCAP3 (1 µg/mL) abolishes GCAP3 immunoreactivity. (E) Addition of purified GCAP1 and GCAP2 (2 µg/mL each) produces minimal decrease in GCAP3 immunoreactivity. *rod outer segments; white arrow, cone cells. Scale bar, 50 µm.

exon 3 amino-acid sequence, although one frame shift, which will cause a nonfunctional translation, was observed. These results indicate that mouse *GCAP3* gene is a nonfunctional pseudogene, which presumably arose originally by duplication of genomic DNA (in contrast to pseudogenes arising by retrotransposition). The mouse *GCAP3* gene may have originally been functional, but low amino acid conservation suggests that this gene became neutralized to a pseudogene during evolution and has diverged without functional constraints (reviewed in ref. Mighell *et al*., 2000).

### Cloning of zebrafish GCAP *cDNAs*

Several expressed sequence tags (ESTs) with homology to human *GCAP*s were found by searching databases with human *GCAP3* sequence using the TBlastx program (http://www.ncbi.nlm.nih.gov/ BLAST/). Primers based on these ESTs were used to amplify zebrafish *GCAP*s by PCR using zebrafish retina cDNA as a template. Three complete cDNAs encoding *zGCAP1*, *zGCAP2*, and *zGCAP3* were amplified. The *zGCAP3* cDNA encodes a protein of 188 amino acids with a calculated molecular mass of 21 868 Da. Correspondingly, the *zGCAP1* and *zGCAP2* cDNA encode proteins of 189 amino acids (21 874 Da) and 197 amino acids (22 956 Da), respectively. The strongest homology was observed within the central region of the protein that encompassed functional EF2 and EF3 $Ca^{2+}$-binding motifs (Fig. 7). The most divergent regions in the amino-acid sequence are located between EF3, the functional EF4 motif, and in the C-terminal region. The N-terminus of mammalian GCAPs was implicated to be crucial for both GC stimulation (Palczewski *et al*., 1994; Li *et al*., 2001) and the conserved N-myristoylation. Zebrafish *GCAP*s contain a consensus myristoylation signal sequence (MGxxxS/E.), where Gly2 is the site of this post-translational modification. The residues around the nonfunctional EF1 motif contains conserved residues, such as W, Y, F, E and P, S, G (Fig. 7) in all *GCAP*s sequenced so far.

### A third subfamily of GCAP*s*: GCAP3*s*

A neighbour joining (NJ)-tree was calculated from vertebrate *GCAP*s and *GCIP*, using vertebrate recoverin and visinin as out-groups (Fig. 8A). The ancestral gene first appears to diverge into *GCIP* and *GCAP* subfamilies, and then *GCAP*s further branched out into three subtypes, *GCAP1*, *GCAP2*, and *GCAP3*. In spite of low identity between human and zebrafish *GCAP3*s (45%) (Fig. 8B), the tree shows the group of *GCAP3*s with high clustering probability (92%). Therefore, we concluded that vertebrate *GCAP3* is a third family of *GCAP*s. Each subtype of *GCAP*s seems to have appeared before teleost-tetrapod divergence. An exhaustive search of the invertebrate database, including *Drosophilae*, did not identify the *GCAP* family of regulators. It is speculated that the *GCAP* gene diverged after vertebrate-arthropod divergence, or is disrupted in other invertebrates. The phylogenetic analysis suggests that amino-acid substitution rates (k) are lower in GCAP1 and GCAP2, than in GCAP3. The *k*-value between zebrafish and human GCAP3 is 0.95, approximately double the *k*-value between zebrafish and human GCAP1 (0.50), and three times higher than the *k*-value between zebrafish and human GCAP2 (0.29). This variation of *k*-values among GCAPs may be because of a difference in the functional constraints. Together, these analyses suggest GCAP3s represent a unique subisoform family of proteins, different from GCAP1s and GCAP2s.

### Biochemical properties of zGCAP3

To measure GCAP-mediated GC activation, zebrafish *GCAP3* was expressed and purified to apparent homogeneity (Fig. 9A). zGCAP3 displayed a minor mobility change in the presence and absence of $Ca^{2+}$, as observed for other GCAPs (Palczewski *et al*., 1994; Gorczyca *et al*, 1994) (Fig. 9A). In the GC assay, GCAPs display the expected properties, modulating ROS GCs in a $Ca^{2+}$-dependent manner stimulating at low and inhibiting at high $[Ca^{2+}]$ (Fig. 9B). zGCAP3 competed with constitutively active GCAP1 [GCAP1(E75Q, E111Q, E155Q)] at high $[Ca^{2+}]$, suggesting that the binding site on GC is similar, if not identical, for GCAP1 and zGCAP3. These biochemical data further demonstrate that this $Ca^{2+}$-binding protein, not only shows sequence relationship to GCAPs, but also shares biochemical properties in stimulating GC, as observed previously for GCAP1 and GCAP2.

### In situ *localization of zebrafish* GCAP *mRNAs*

Zebrafish photoreceptor cells are categorized morphologically into five types (Fig. 10B): rods, two different cones from the double cone pairs (DC), long single cones (LS), and short single cones (SS) (Raymond *et al*., 1993). The nuclei of DC and LS protrude above the external limiting membrane and the nuclei of SS and rods remain below it. The distribution of zebrafish *GCAP* mRNAs was investigated by *in situ* hybridization. The digoxigenin labelled *zGCAP3* antisense RNA probe hybridized specifically to the myoid region of cone photoreceptors (Fig. 10A, left). Signals were observed in cell bodies of LS, SS and both members of DC (Fig. 10B). Cone cells negative for the *zGCAP3* antisense RNA probe were not identified in our experiment. As a control, *zGCAP3* sense RNA probe did not show hybridization signals (Fig. 10A, right). These results suggest that *zGCAP3* is expressed in all four types of cone photoreceptors, but not in rods. Figure 10C and D shows the localization of *zGCAP1* and *zGCAP2* mRNAs, respectively. In both cases similar patterns were observed. Hybridization signals were observed only in the photoreceptors whose cell bodies are below the external limiting membrane. Signals were observed in the cell bodies and myoid regions of rods, as well as in the myoids of SS (see arrows in Fig. 10C and D, left). Signals were not observed in DC and LS whose nuclei are beyond the external limiting membrane. SS negative with GCAP1/2 antisense probes were not observed in these sections. Unlike human *GCAP2* expression, no staining was observed in inner retinal neurons for *zGCAP1* or *zGCAP2*. As a similar expression pattern and intensity was observed for *zGCAP1* and *zGCAP2*, RNA dot blots were employed to test the specificity of RNA–RNA hybridization. Unlabelled sense transcripts of *zGCAP*s were blotted onto hybond NX membrane and hybridized under the same condition as *in situ* hybridization, using *GCAP* antisense probes. Each *zGCAP* antisense probe hybridized specifically to corresponding *zGCAP* sense transcript (Fig. 10E). These results indicate that the hybridization conditions employed here are specific, verifying that *zGCAP1* and *zGCAP2* are coexpressed in rods and SS, but not in other cone photoreceptors.

### Evolutionary trace analysis of the GCAP family

ET analysis was performed on the GCAP family consisting of 33 members. ET uses the sequence identity tree for the family as a means of dividing the multiple sequence alignment into distinct subclasses that are then examined for patterns of amino acid conservation and variation (Lichtarge *et al*., 1996). Residue positions that have an invariant amino acid within each subclass, but whose identity varies among the subclasses, are termed class-specific and have been shown to impart functional specificity among family members (Sowa *et al*., 2000). When the GCAP family is divided in such a way that GCAP1, GCAP2, GCAP3, and GCIP form subclasses, class-specific residues emerge on each of the EF-hands and form clusters at multiple sites on the surface (Fig. 11A and B)
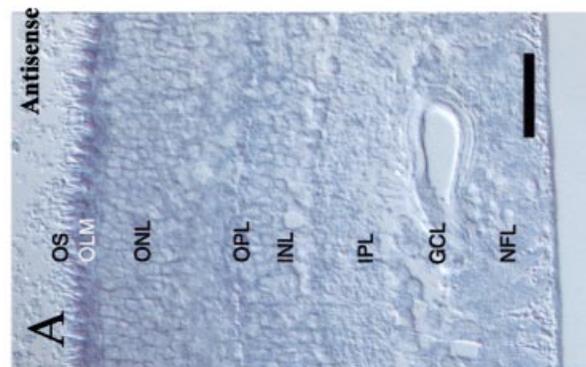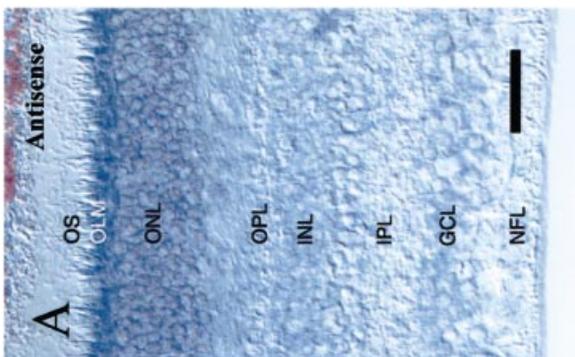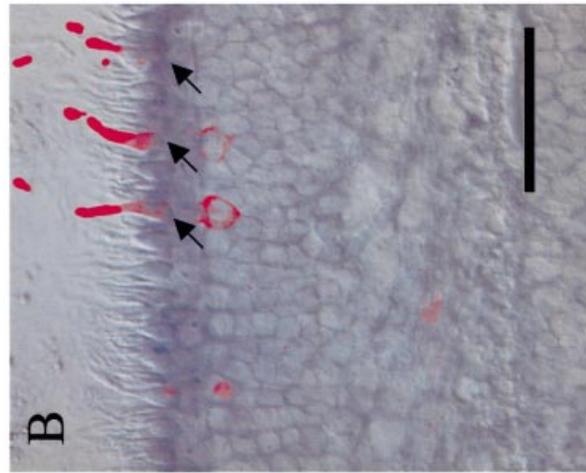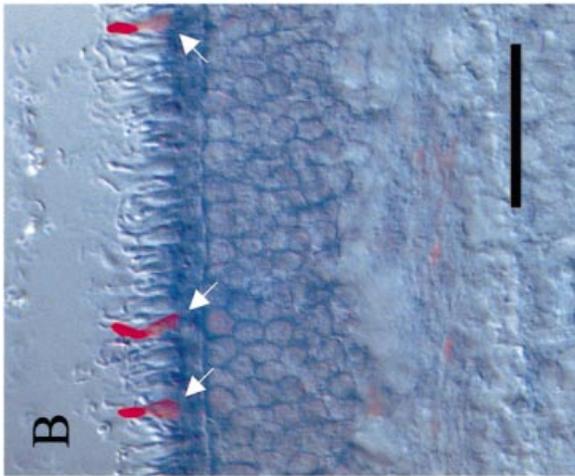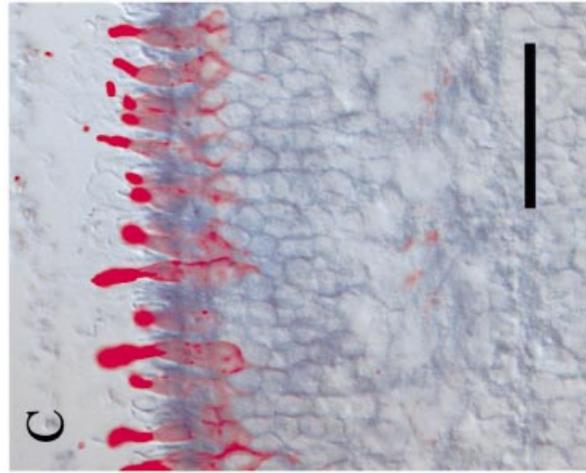
Fig. 4.



Fig. 5.

when mapped onto the Ca$^{2+}$-bound structure of GCAP2 (Ames *et al.*, 1999). Residue numbers in Fig. 11 and in the discussion below are based on bovine GCAP1.

The largest surface cluster comprises residues from EF1 and EF2. They include class-specific residues His19, Lys23, Lys24, Gln33, Leu34, Thr35, Phe42, Phe43, Tyr55, Met59, Phe63, Asn66, Lys67, Phe68, Gly69, Tyr70, Met74, Ala78, Leu80, Ser81, Leu82, and Val83. They also include the invariant (within the GCAP family)

residues Trp21, Tyr22, Phe25, Glu28, Pro30, Ser31, Glu38, Asp68, Asp72, Phe73, and Glu75. Residues from this region have previously been proposed to play a role in regulating guanylate cyclase (Otto-Bruc *et al.*, 1997; Ames *et al.*, 1999; Li *et al.*, 2001), and the residues Phe73–Glu75 were shown to be critical for GC activation (Schrem *et al.*, 1999). Olshevskaya *et al.* (1999) have reported that replacing residues Phe78 to Asp113 in GCAP2, with the corresponding region from neurocalcin, produces a chimera that activates GC at high Ca$^{2+}$

## A

```
mGCAP3: atgctagcttcattttacagtgaagaatgaaggtctacaccaagagataatttatacaaa 108
        ||| ||||| || |||| || |||| ||||| |  | ||||||   |      ||
hGCAP3: atgttagccttcagttttagtgaggagtaagggactaaatccagcaaaaacttaagtgaa

mGCAP3: accaacctgagcaaaaggctgggttctgagaatcATGTCCGGGATCATTGGATCCATACC 168
        ||||||||| |||| |  |  | |||||| ||| ||  ||||  || ||  ||
hGCAP3: aacaacctgaggaaaa-gctgtagactgtgagtcaagATGGGGAATGGCAAATCTATAGC

mGCAP3: TGATGATAAGACAGCAATTCCT--CAAAGAGACCTGTGAGTGGCATAGAGCCTTTAAGAT 226
        || |||| ||| ||| ||  |    |||||||   ||||| ||||  || ||||| ||||
hGCAP3: TGGTGATCAGAAAGCAGTTCCTACACAAGAGACCCATGTGTGTACAGAACATTTATGAT

mGCAP3: GGAACTCCTGCCCCGCCTGTGAACACTGCATAAACGAAAG--CATTTTGGGTTGGTGAGG 284
        ||||  || || ||||||||||| ||| ||  || ||||    ||||||||| ||||||
hGCAP3: GGAATATCCATCCGGCCTGCAAACACTACATGAATTTAAGCACACTTTTGGGTCTGCAAGG

mGCAP3: TCTGTAGCA-AAGGCCAATCAACA---AGATCAAGTTTATAATGCCTTCATTATGACCCT 340
        ||||| ||  |||||||||| ||    | |||||||||| ||| ||||||| ||||||||
hGCAP3: TCTGAATCAGAAAGGCCAATAAACATATTGATCAAGTTTATAATACCTTTGACACGAACAG

mGCAP3: Ttgcttttcatt
        || ||
hGCAP3: Ggtaagatcttt
```

**Exon 1**

## B

```
mGCAP3: cttcacacaacccaccgtgtgcaggtgagccagtcattttaaacacgtttagcattggcga 485
        ||||| |||| ||| ||| | || |||  || ||||| |||| | ||||  ||| ||
hGCAP3: cttcaggcaactcacagcttgtaggtaagtgagtca-ttaaatactttttagtactgacgg

mGCAP3: catgaaataattggaaaatcgcctct-ctaccctttggaaatgttctgcatgtagagagt 544
        |||||||||||| ||||  | ||||| | ||| || |||||| || ||||||  | |||||
hGCAP3: catgaaataattgggaactagcctctcccaccctaggaagtgttctgcatgtagggagt

mGCAP3: gatttt--aaaccaaattaagtctcagcatggaatctaatgctatcgtttaaataaatct 603
        ||||||   |||||||| |||||| |||||||||||| ||||||||||| |||||||||||
hGCAP3: tattttaaaaaccagattaaatctcggcatggaattctaatgctatcatttaaataaatct

mGCAP3: aatacgtgcaaattgattacagagactgtttgcaaagtatgtaatgcattggtgacatt 663
        |||| || || ||| | |||| ||||| || ||||| ||||||| || ||||||||||||
hGCAP3: aataagtacagattgattcatacaaagactgttttcgaagtatttaatgcattggtgacatt

mGCAP3: ttatcaaaaggcagattgaggggcttgcttttaaaagtgtgattatatctagtttggca 723
        |||| ||| || |||| ||  | |||||||||| ||||||||| ||| ||||||| ||||
hGCAP3: ttatagaaaagcaaattacaggactctgcttttaaaagtgtgattgcatctcagattggca

mGCAP3: gataaatcaatacaaattagccaatgtggtgtc 757
        ||||| ||||||||| ||||||| ||  || ||
hGCAP3: gatataatcaatacaaattagccaacatgttgtc
```

**Intron A**

## C

```
MGCAP3: caattcatttaatttctaagcttcattactaagtac-cacatatgatgtttcatcctagt 101
        || |||||||||| ||||| ||||  |   | |||     ||||| | ||||| |   |
HGCAP3: cagttcatttaatttccaagtctcattacccagaactgacatacaatcttttctttttat

MGCAP3: ----ttttaaaagctagaacaggttaggaagcaaaacttataccaacacattgcccaaat 157
        ||| | |  |  ||| |  ||||||| | |   |||| ||  ||| |  |
HGCAP3: ttactttttaacaactggtacaggttggatagcaa------ccgacaacacatccccaaatt

MGCAP3: ctatcacattggcatagaaatgctgcagaaagcatttgcatccagcaaagttgaactc-- 215
        || |||||| |||| || |   ||||| |||   ||| | | |||| ||||| || |
HGCAP3: ctgtcacatcggagcagaaatgttgcaaaatgtatttgcttccagaaaagttgacctctt

MGCAP3: --------tgcttgcttgcagGCTGTTCAAGCCCTCAACAGCCAGAAACCTCTAAGTCTT 267
        | |  ||  | |||||| ||  |||||| ||||| |  ||||  || || |
HGCAP3: tcatttaatgtcttttgcagGCGGTTACAAGCCCTCAATGGCCAGCAAACTCTGAGTCCT

MGCAP3: GAGGCCTTTA-CAACATGGTTGCTTCATAATATTGACATAGAC 308
        || |  |||| || ||| ||||| ||| |||| |  | |||||
HGCAP3: GAAGAATTCATCAACTTGGTGTTCCATAAGATCGATATAAAC
```

**Intron C**

**Exon 3**

## D

```
Exon 1
                                    ↓            EF1        ↓         ↓
MGCAP3: MSGIIGSIPDDKTAIPXKETCEWHRAFKMELLPRL*TLHKRKXILGW*GL*XKANQXXDQ 60
        | ||  | | ||    | |||| ||  | ||    |  || ||  | ||  ||
HGCAP3: M-GNGKSIAGDQKAVPTQETHVWYRTFMMEYPSGLQTLHEFKTLLGLQGLNQKANKHIDQ 59

        EF2
MGCAP3: VYNAFIMTL 69
        ||| |
HGCAP3: VYNTFDTNK 68
```

```
Exon 3 (partial)                         ↓          EF4

MGCAP3: AVQALNSQKPLSLEAFXNMVLHNIDID 27
        ||||||  | | ||||  | || ||
HGCAP3: AVQALNGQQTLSPEEFINLVFHKIDIN 27
```
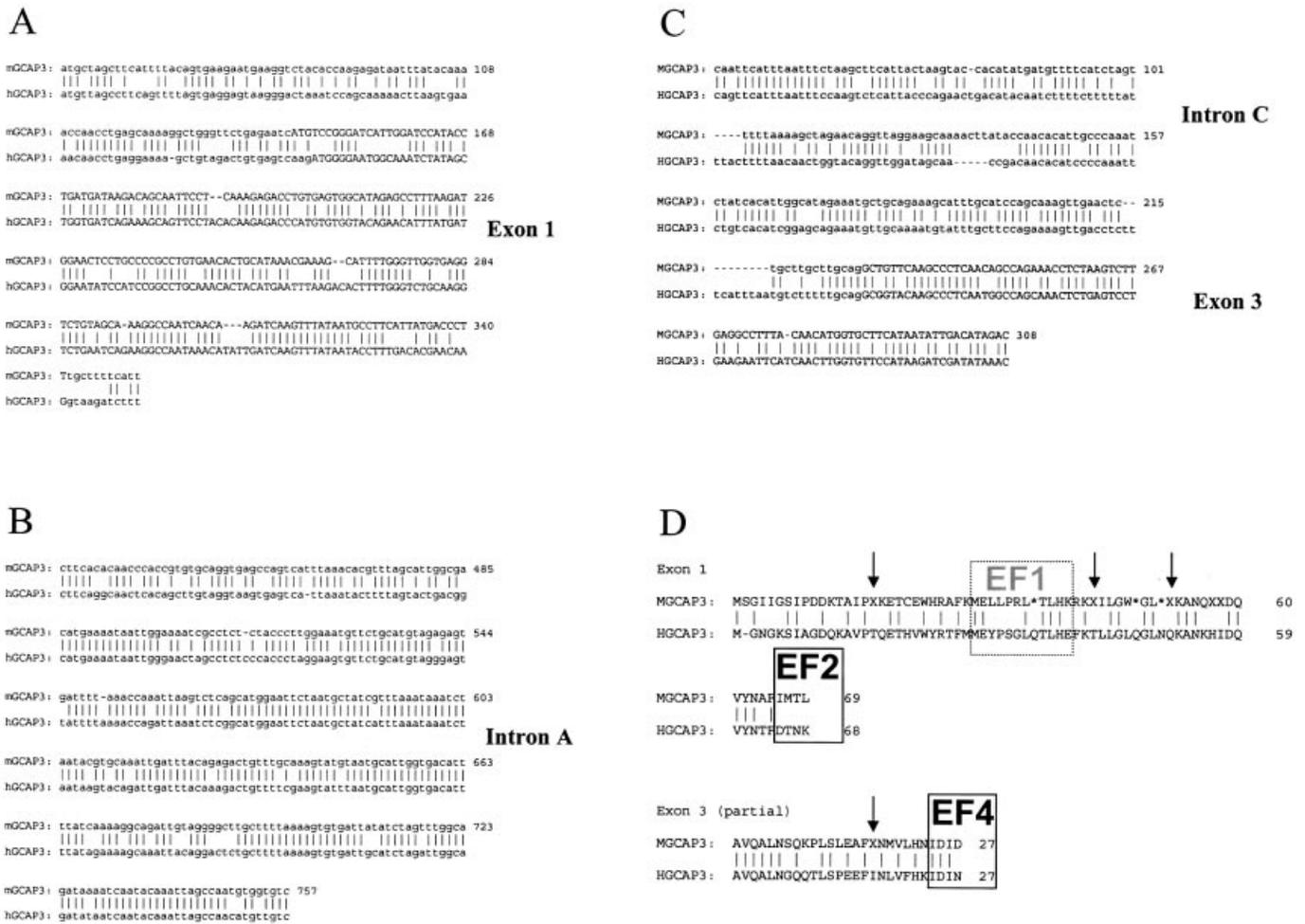
Fig. 6. Partial gene sequence exon/intron junction of *mGCAP3* compared to *hGCAP3* gene. Vertical bars indicate the positions of identical residues. Exons are shown in capital letters. (A) Comparison of mouse and human *GCAP3* genomic sequence around exon 1. In this region 67% of nucleotides (195/288 nucleotides with 9 gaps) were identical and 72% of nucleotides (128/177 nucleotides with 8 gaps) are identical in exon 1. (B) Comparison of mouse and human *GCAP3* genomic sequence of intron A. In this area, 83% of nucleotides (279/334 nucleotides with three gaps) are identical. Note that sequence of A. and B. is from one contiguous genomic fragment. (C) Comparison of mouse and human *GCAP3* genomic sequence including partial exon 3 region. In this region, 69% of nucleotides were identical (196/282 nucleotides with 21 gaps). Especially high identity (75% 61/81 nucleotides with 1 gap) was observed in exon 3 region. (D) Comparison of translated sequence. Frame shift sequences are translated into X residues. Arrows indicate positions of frame shifts due to deletion in *mGCAP3* gene. The nonfunctional EF1 hand in human *GCAP3* is boxed by broken line. The EF hand motifs (EF2 and 4) in human GCAP3 are boxed.

---

Fig. 4. *In situ* hybridization of human GC1. (A) *In situ* hybridization of GC1 transcripts using antisense (left) and sense (right) RNA. The strongest signal is in cone inner segment and cell bodies. Rod inner segments and cell bodies were also strongly labelled. Inner nuclear neurons and ganglion cells are weakly labelled. (B) Double labelling with anti-blue cone opsin. Anti-blue cone opsin labels cone photoreceptors (red) which hybridizes GC1 cRNA probe (blue). (C) Double labelling with anti-red/green cone opsin. Red/green cones (red) are labelled with GC1 cRNA (blue). White arrows, blue cones. Scale bar, 50 μm.

Fig. 5. *In situ* hybridization of human GC2. (A) *In situ* hybridization of GC2 transcripts using antisense (left) and sense (right) RNA. Strong signal is observed in cone inner segments. Rod inner segments and cell bodies were weakly labelled. (B) Double labelling with anti-blue cone opsin. Anti-blue cone opsin labels cone photoreceptors (red) which hybridizes with GC2 cRNA probe (blue). (C) Double labelling with anti-red/green cone opsin. Red/green cones (red) are labelled with GC2 cRNA (blue). Black arrows, blue cones. Scale bar, 50 μm.
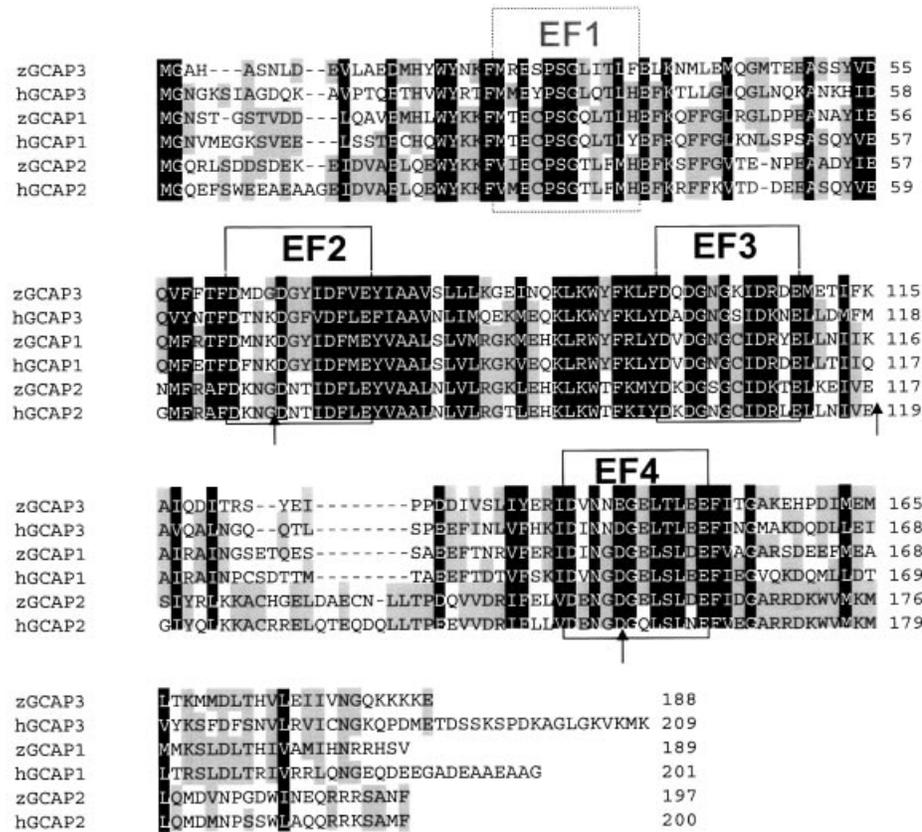
FIG. 7. Amino-acid sequence alignment of *Homo sapiens* (prefix h) and *Danio rerio* (prefix z) *GCAPs*. The three EF hand motifs (EF2–4) representing high affinity Ca²⁺ binding sites are boxed. The nonfunctional EF1 hand is boxed by a broken line. Residues conserved in all GCAPs shown here are printed white on black. Residues not uniformly conserved are shaded. Arrows indicate the positions of introns in the three human *GCAP* genes whose exon/intron arrangement is identical (Surguchov *et al.*, 1996; Haeseleer *et al.*, 1999).

concentrations and inhibits it at low concentrations. Within this region (Phe73 to Asp108 in GCAP1), 12 residues are identified as class-specific and cluster primarily on the exiting helix of EF2. The region from Lys29 to Phe48 in GCAP2 (Lys23–Phe42 in GCAP1) is involved in GC activation and inhibition (Olshevskaya *et al.*, 1999) and contains five class specific residues, four of which are solvent accessible and therefore could interact with GC.

The second cluster is composed predominantly of residues from EF3, with some contribution from EF4. One face of the exiting helix of EF3 is composed entirely of class-specific residues (Leu112, Ile115, Ile116, Ile119, Arg120, Ile122, and Asn123), yet this face does not interact with the entering helix of EF2 indicating that these class-specific residues may mediate some other interaction besides structure stabilization. Residues in the region spanning Phe170 to Asn189 in GCAP2 were shown to help mediate GC activation (Olshevskaya *et al.*, 1999), yet the only ET-identified residues in this area are invariant across the GCAP family, and are located primarily on the exiting helix of EF4. However, one face of the entering helix of EF4 is composed of four class-specific residues that are positioned to interact with the C-terminal helix of GCAP2.

### Evolutionary trace analysis of the NCBP family

An ET of the entire neuronal Ca²⁺-binding protein (NCBP) family, including the GCAPs, calsenilin, neurocalcin, recoverin, visinin, and frequenin families (106 sequences total) reveals a similar pattern of class-specific residue clustering to the ET of the GCAP family, yet several differences emerge (Fig. 11C and D). The almost complete lack of EF1 class-specific residues and the lower number of residues from EF2 in the NCBP trace indicates that the evolutionary importance of this region is specific for the GCAP family and is likely not to play a major role in other members of the NCBP family.

The stretch of class-specific residues including Met59, Tyr55, Ile122, Ile119, Asn123, Ile116, Arg120, and Phe135, is the same for both the GCAP trace and the NCBP trace, indicating that this region from EF2 and EF3 has importance for the entire NCBP family. The pattern of class-specific residues located within the protein is almost the same in the NCBP and GCAP traces, with the exception of EF1 and the exiting helix of EF2. For example, the exiting helix of EF3 has the same face composed entirely of class-specific residues in both the NCBP and the GCAP traces. The entering helix of EF4 also shares the same pattern of class-specific residues in both traces. In the NCBP trace, the entering helix of EF2 shares four of the five class-specific residues found in the GCAP trace, indicating that these residues may be structurally important for the formation of the cleft created by this helix and the EF3 domain. It is not surprising that the class-specific internal residues in both traces are nearly identical, yet the fact that these residues are class-specific suggests that changes to the internal architecture of the protein could have effects on the functional specificity of individual family members.

## Discussion

### Pairing GCAPs and GCs: cell type gene expression and protein localization

In human retina, *GCAP1* and *GCAP2* are expressed in both rod and cone photoreceptors (Fig. 1B and C), whereas *GCAP3* is expressed in all types of cones, but not rods, and localizes to cone outer segments (Figs 1–3). In contrast, GC1 and GC2 are present in both rods and cones (Figs 4 and 5). These results suggest that four GC/GCAP pairs are possible in rods, whereas six pairs are feasible in cones.
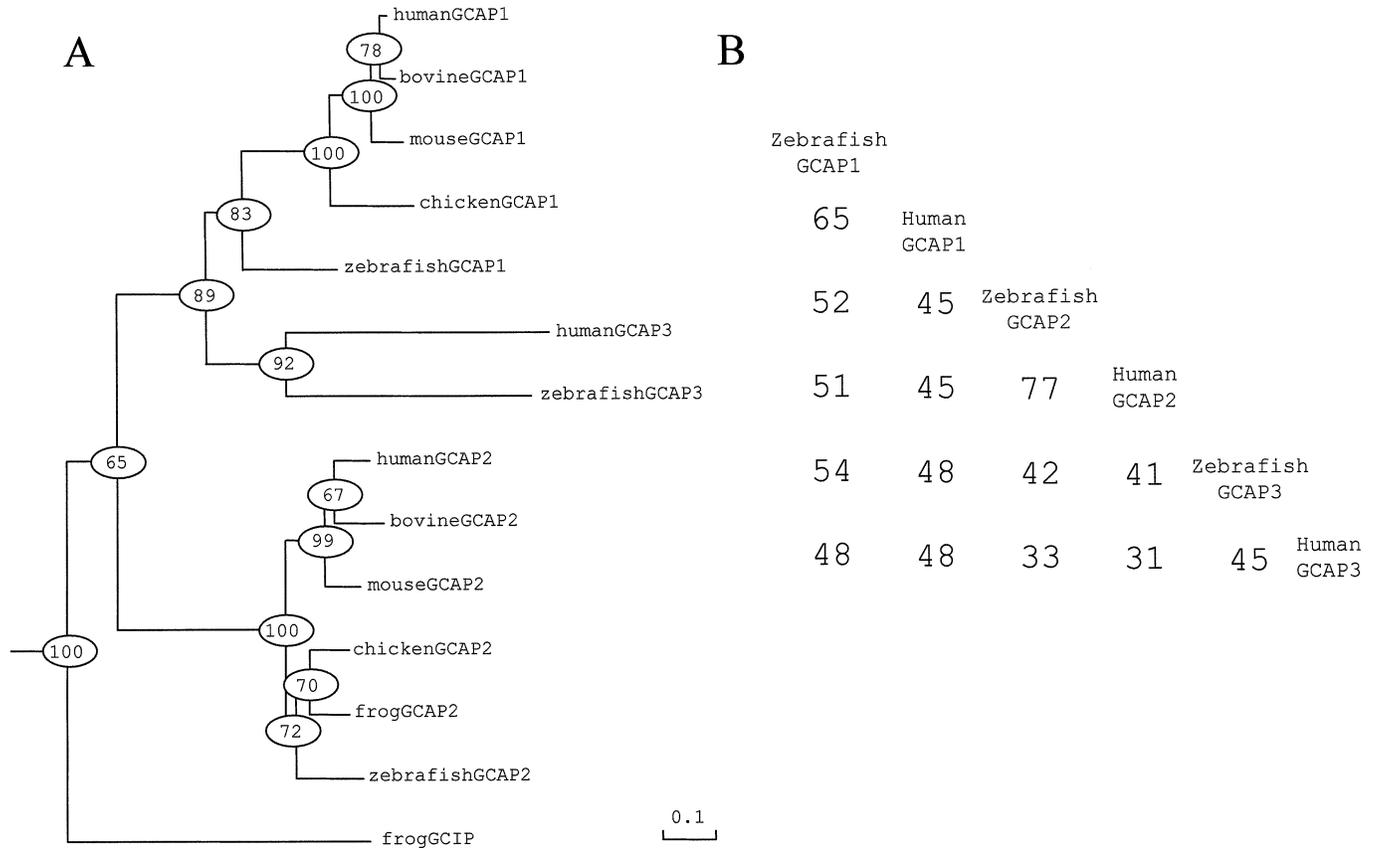
FIG. 8. A phylogenetic and amino acid identities of GCAPs. (A) A phylogenetic tree calculated from the amino-acid sequences of GCAPs. Numbers indicate clustering percentage obtained from 1000 bootstrap resamplings. Bar indicates 10% replacement of an amino acid per site (k = 0.1; see Material and methods). (B) The amino acid identities between GCAPs from ClustalW alignment. Gaps were taken as the same amino acid. Sequence data used in the present analyses were taken from GenBank, EMBL, SWISS-PROT, NCBI databases, except for mouse *GCAP2* (Howes *et al.*, 1998). Accession numbers are as follows: human *GCAP1* (11417667), bovine *GCAP1* (1169873), mouse *GCAP1* (1169875), chicken *GCAP1* (5713275), human *GCAP3* (6226818), human *GCAP2* (8928106), bovine *GCAP2* (1730238), chicken *GCAP2* (5713277), frog *GCAP2* (6225434), and frog *GCIP* (AAC15878).
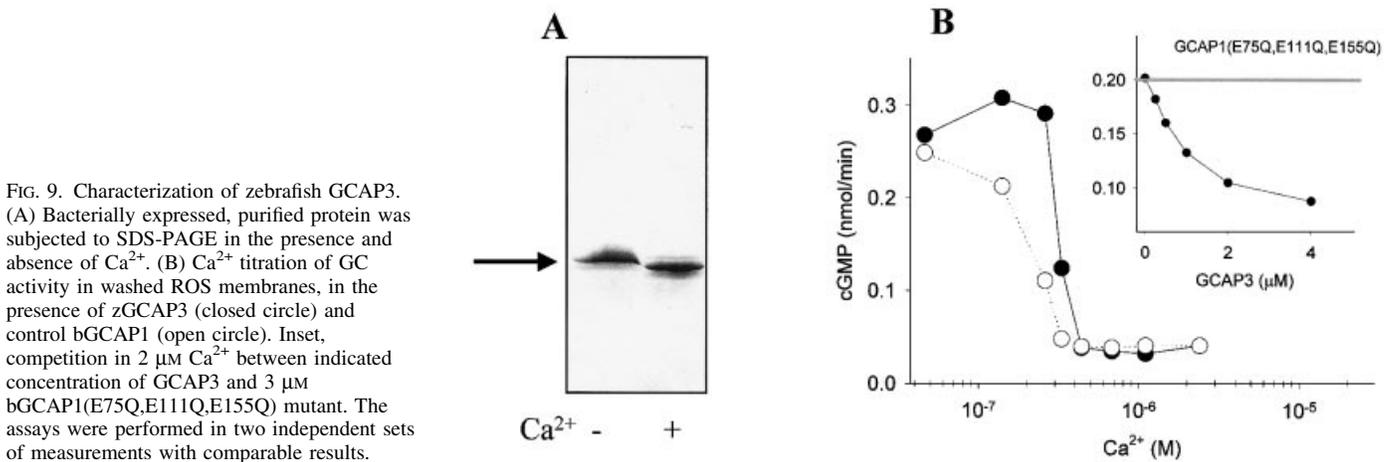


FIG. 9. Characterization of zebrafish GCAP3. (A) Bacterially expressed, purified protein was subjected to SDS-PAGE in the presence and absence of $Ca^{2+}$. (B) $Ca^{2+}$ titration of GC activity in washed ROS membranes, in the presence of zGCAP3 (closed circle) and control bGCAP1 (open circle). Inset, competition in 2 μM $Ca^{2+}$ between indicated concentration of GCAP3 and 3 μM bGCAP1(E75Q,E111Q,E155Q) mutant. The assays were performed in two independent sets of measurements with comparable results.

Localization of GCAPs was extended to zebrafish. GCAP1 and GCAP2 localized to rod cells and SS, whereas GCAP3 was found in all subtypes of cones. Four members of sensory organ specific membrane GC (OlGC-R1, OlGC-R2, OlGC-C, OlGC3) were found in teleost fish (Seimiya *et al.*, 1997; Hisatomi *et al.*, 1999). *In situ* hybridization located OlGC-R1 and OlGC-R2 in rods, and OlGC-C in cones (Hisatomi *et al.*, 1999). OlGC-3 transcripts were localized in

photoreceptor cells (Kusakabe & Suzuki, 2001), but it is unclear in which cell type. Therefore, teleost fish may have a different combination of GC-GCAP pairs in rods and cones.

Expression levels of different GCAPs and GCs in rods and cones vary more among species than those of any other known phototransduction enzymes. The diversity of GCAP-GC pairing could be an important mechanism underlying observed differences
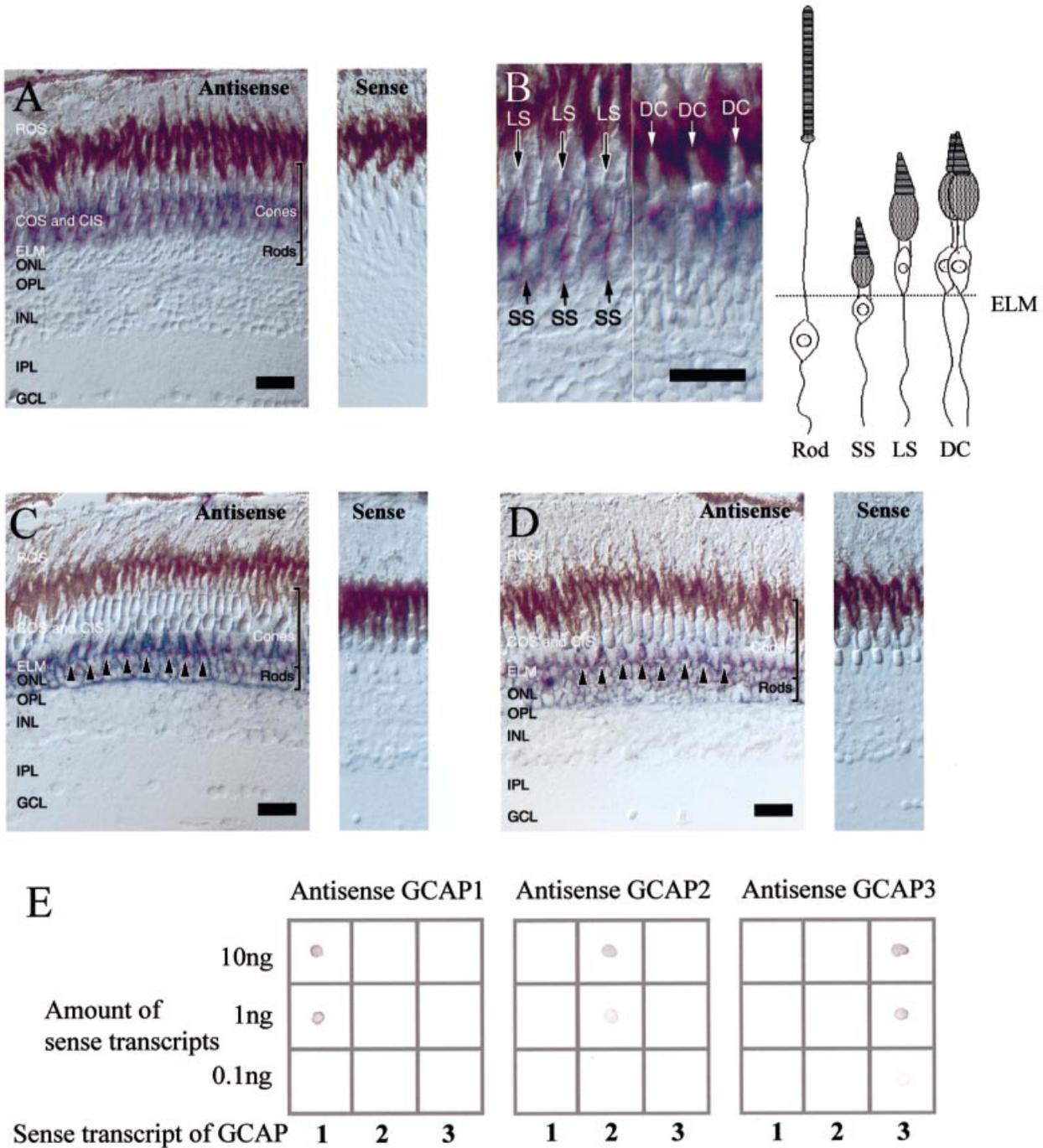
FIG. 10. *In situ* hybridization of zebrafish GCAPs and specificity of hybridization. (A) *In situ* hybridization of GCAP3 transcripts using antisense (left) and sense (right) RNA. The strong signal is in cone inner segment. No signal is observed in rod myoid or cell bodies. (B) Localization of *GCAP3* mRNA with higher magnification. Signals are observed in short single cones (SS), long single cones (LS), and double cones (DC). (C) *In situ* hybridization of GCAP1 transcripts using antisense (left) and sense (right) RNA. SS were strongly labelled (arrowheads). Rod myoids and cell bodies are also labelled. (D) *In situ* hybridization of GCAP2 transcripts using antisense (left) and sense (right) RNA. SS were strongly labelled (arrowheads). Rod myoids and cell bodies are also labelled. Abbreviations: ROS, rod photoreceptor outer segments; COS, cone photoreceptor outer segments; ELM, external limiting membrane; ONL, outer nuclear layer; OPL, outer plexiform layer; INL, inner nuclear layer; IPL, inner plexiform layer; and GCL, ganglion cell layer. Scale bar, 20 μm. (E) RNA dot blots of zebrafish GCAP transcripts. Different amounts of GCAP sense transcripts (0.1, 1, and 10 ng) were blotted on Hybond-NX membrane. *GCAP1* cRNA probe hybridized specifically to GCAP1 sense RNA blotted on left column (left). GCAP2 hybridized to GCAP2 sense transcripts blotted on middle column (middle). GCAP3 antisense probe hybridized to GCAP3 sense transcripts blotted on right column.

among animal groups in their electrophysiological responses, such as implicit times, light sensitivity, light adaptation, and rate of dark adaptation (Dowling, 1978; Baylor, 1987; Rodieck, 1998).

*Pairing GCAPs and GCs: human and mouse physiology*

Insight into the functions of GCAPs and GCs in phototransduction can be gained from naturally occurring mutations and engineered
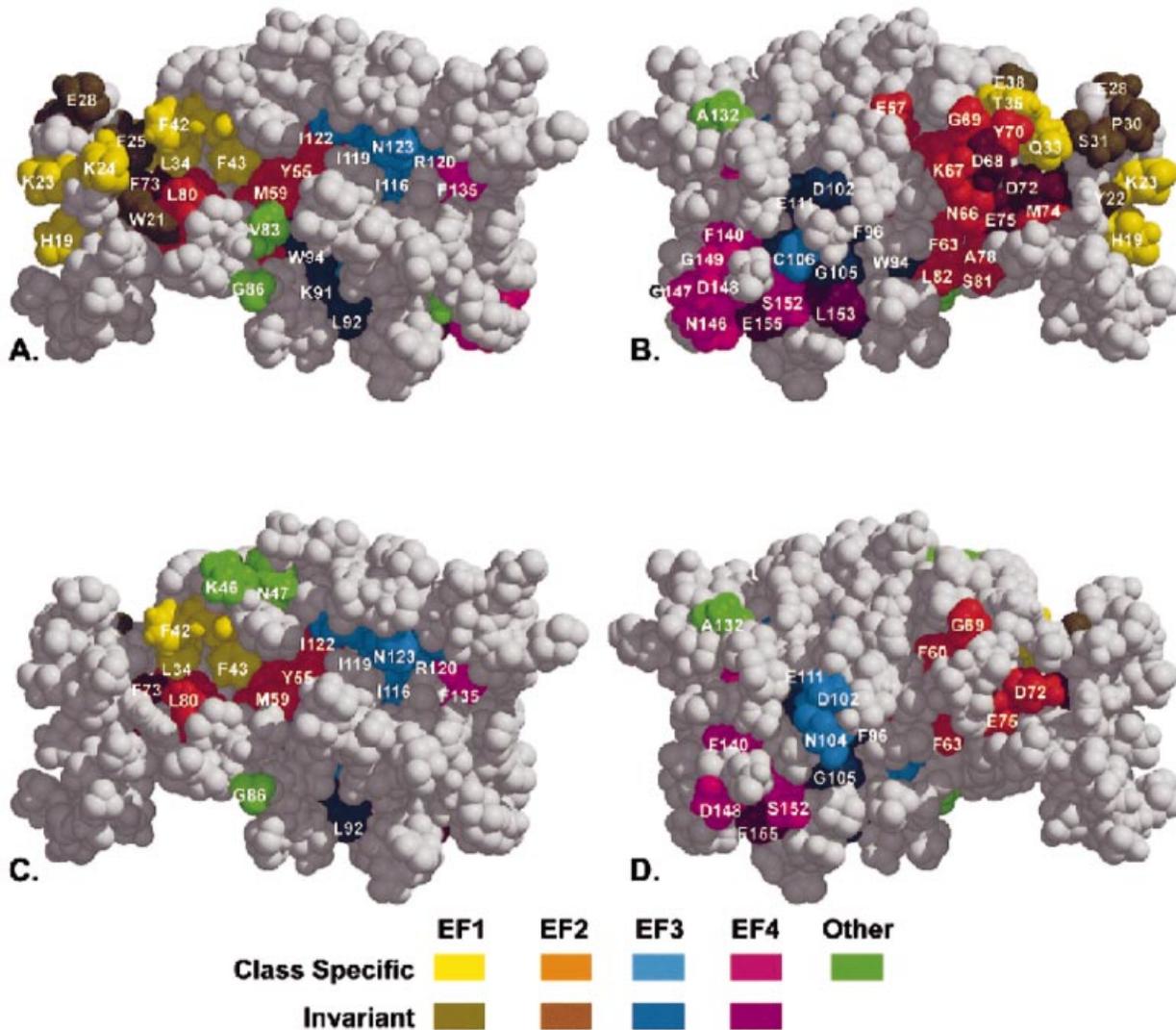
FIG. 11. Evolutionary trace analysis of the GCAP and NCBP families. An Evolutionary trace analysis (ET) was performed on both the GCAP family (33 members) and the NCBP family (106 members, including the GCAP subfamily). The results were mapped onto the structure of $Ca^{2+}$-bound GCAP2 (Ames *et al.*, 1999). EF hands, class specific, and invariant residues are coloured according to the colour table, with numbering and amino acid designation based on bovine GCAP1. Views A and B are rotated 180° about the *y*-axis with respect to each other as are C and D. (A, B) ET analysis of the GCAP subfamily reveals a large surface cluster of both class specific and invariant residues from EF1 and EF2. This site is much smaller in size for the NCBP trace suggesting that this region is specific for the GCAP subfamily (A vs. C, B vs. D). The stretch of ET-identified surface residues beginning with Phe73 and ending with Phe135 (A vs. C) is found in both the NCBP and the GCAP traces, indicating that this site is important for the functional specificity of the entire NCBP family.

gene disruptions. A dominant form of human retinal degeneration originating in cones results from mutations in *GCAP1* (Payne *et al.*, 1998) that lead to high activity of GC even at $[Ca^{2+}]$ that normally inactivate GCAP1 (Dizhoor *et al.*, 1998; Sokal *et al.*, 1998). There was no severe degeneration of rods reported in these patients. This is likely due to either lower expression levels of GCAP1 in human rods as compared to cones (Fig. 1B), instability of the mutant protein in rods, or because of a lower sensitivity of rods than cones to imbalances on $Ca^{2+}$-homeostasis. Inactivation of GC1 in humans leads to recessive Leber Congenital Amaurosis (LCA), an early onset rod and cone degeneration, that causes initially very limited vision and ultimately leads to total blindness (Perrault *et al.*, 1996; Perrault *et al.*, 2000). This phenotype is consistent with that observed for a naturally occurring *GC1* mutation in chickens (Semple-Rowland *et al.*, 1998). A missense

mutation (E837D) in *GC1* was identified in family members affected with LCA, and a second missense mutation (R838C) was identified in other families with dominant cone–rod dystrophy (Kelsell *et al.*, 1998; Van Ghelue *et al.*, 2000). It was reported that the *R838C* mutant shows reduced overall catalytic efficiency, reduced stimulation by GCAP2, and an increase in the apparent affinity for GCAP1, as well as a shift to higher $[Ca^{2+}]$ of the GCAP1 $Ca^{2+}$-sensitivity. These results point out functional differences of GCAP1-GC1 pairs in both rod and cone cells (Tucker *et al.*, 1999). It was suggested that some other mutations affect the connection of photoreceptors to secondary neurons as GC1 is also found in synapses (Gregory-Evans *et al.*, 2000). Although no disease has been associated with GC2 mutations, the expression of this cyclase in rods and cones suggests the importance of this protein in scotopic and photopic vision.

Further genetic manipulation and electrophysiological measurements are required for additional insight into the role of this cyclase.

Disruption of the *GC1* gene in mice does not lead to changes in the level of GC2, suggesting that the expression of one cyclase is independent of the second (Yang *et al.*, 1999). The a- and b-waves of electroretinograms (ERG) from dark-adapted null mice were suppressed markedly, suggesting a major deficiency in signal transduction. Cones, which are only ≈3% of all murine photoreceptor cells (Carter-Dawson & LaVail, 1979; Applebury *et al.*, 2000), are initially present at normal levels in the retina but disappear by 5 weeks in *GC1*-null mice (Yang *et al*, 1999). Surprisingly, rods isolated from these mice, despite having a normal dark current, recovered from a light flash markedly faster in single cell recordings.

Mice lacking both *GCAP1* and *GCAP2* have altered light responses as measured by ERG and single cell recordings (Mendez *et al.*, 2001). The GC activity from GCAPs$^{-/-}$ ROS showed no Ca$^{2+}$-dependent modulation, indicating that Ca$^{2+}$ regulation of GCs had indeed been abolished. Rod flash responses from dark-adapted GCAPs$^{-/-}$ rods were larger and slower than responses from wildtype rods, consistent with absence of GCAP3 in mouse. *GCAP1*, but not *GCAP2*, restored wildtype responses when expressed on the GCAPs$^{-/-}$ background (W. Baehr, K. Howes, M. Pennesi, F. Rieke, K. Palczewski and P. Detwiler, unpublished results), suggesting that GCAP2 is dispensable for the rod function.

### GCAP3–a cone specific isoform of GCAPs

Rods and cones are known to have similar isozymes of various transduction proteins including opsins, transducins, phosphodiesterases, cGMP-gated channels, and arrestins. The molecular properties of these isozymes result in the physiological differences between rods and cones, such as sensitivity and adaptation processes. Among NCBPs, only visinin and s26, a homologue of recoverin (Goto *et al.*, 1989; Kawamura *et al.*, 1996), and GCAP3 have been reported to be cone specific. However, it was proposed that visinin and s26, found only in nonmammalian species, are not necessary for normal mammalian cone physiology because recoverin is expressed in rods and cones of mammalian photoreceptors (Polans *et al.*, 1993). In this study, we show that zebrafish and human possess a cone specific GCAP isoform, GCAP3, which likely contributes to cone-specific features of [Ca$^{2+}$] homeostasis, and GC regulation. GCAP3s are predicted to have three functional EF-hands for binding of Ca$^{2+}$, and a consensus sequence for N-myristoylation at Gly2. Both GCAP3s can activate photoreceptor GC (Fig. 9B) (Haeseleer *et al.*, 1999), and hGCAP3 has been shown to stimulate both GC1 and GC2 *in vitro* (Haeseleer *et al.*, 1999), suggesting overlapping functions of all three GCAPs in regulation of cone photoresponses.

The human *GCAP1* and *GCAP2* genes are arranged in a tail-to-tail array on chromosome 6p (Surguchov *et al.*, 1996), while the *GCAP3* gene is located on 3q13.1. Chicken and mouse have also conserved the tandem array of these genes. The close relationship between *GCAP1* and *GCAP3* (Fig. 8) suggests that the *GCAP3* gene translocated after formation of the *GCAP1/2* tandem array. However, we were unable to demonstrate (by long range genomic PCR) that a tail-to-tail *GCAP1/2* gene array exists in zebrafish, so it is possible that the *GCAP1/2* are on different chromosomes in this species. Our finding of three GCAPs in zebrafish retina suggests that these gene duplication and translocation events occurred prior to vertebrate diversification.

We were unable to detect *GCAP3* cDNA in mouse and bovine retina by RT/PCR and library screening, although the bovine *GCAP3* gene was detectable by Southern blot analysis (Haeseleer *et al.*, 1999)

Based on our sequence analysis, it appears that the mouse *GCAP3* gene is inactive (Fig. 6). This conclusion is supported by our observation that the retina from knockout *GCAP1/GCAP2* mice appears to lack GCAP3 as tested using immunoblotting with generic anti-GCAP G2 antibody (data not shown).

### GCAPs – key residues for the function and structure

The ET analysis reveals two major clusters of functionally important residues for members of the GCAP family. The first is largely from EF1 and EF2, and the second includes primarily residues from EF3, with some contribution from EF4. These regions have been previously implicated in GC regulation and may be directly involved in GC binding. While most of these positions are also identified by the ET as important for the entire NCBP family, the functional importance of much of the EF1/EF2 cluster appears unique to the GCAP family. Therefore these residues likely emerged early in the evolution of GCAPs as sites important for regulation of GC. The theoretically identified residues are in agreement with recently determined key regions of GCAP1 that are involved in the interaction with photoreceptor GC (Li *et al.*, 2001; Sokal *et al*, 2001).

In summary, our results demonstrate that *GCAP1*, *GCAP2*, *GC1* and *GC2* are expressed in human rod and cone photoreceptors, but *GCAP3* is expressed exclusively in red/green and blue cone photoreceptors. Furthermore, we identified all three GCAPs from teleost fish (zebrafish) retina and localized them to rods, SS (GCAP1 and GCAP2), and all-subtypes of cones (GCAP3), suggesting that GCAP3 is not primate specific as suspected previously. An extensive modification of the *GCAP3* gene explains why this transcript/protein is not produced in mouse retina. Mouse is a nocturnal animal in which cone vision plays a minor role as compared to human or fish. Sequence comparisons in conjunction with functional testing of the different GCAPs allowed us to identify key conserved residues that are critical for GCAP structure and function. The importance of these proteins in phototransduction is proven; however, many specific questions still require further analysis. This study provides important novel data on the paring of GCs and GCAPs and in depth characterization of GCAP3 from zebrafish to man.

### Abbreviations

AP, alkaline phosphatase; CaM, calmodulin; DC, double cones; ERG, electroretinogram; EST, expressed sequence tag; ET, evolutionary trace analysis; GC, guanylate cyclase; GCAP, GC-activating protein; GCIP, GC-inhibitory protein; LCA, Leber Congenital Amaurosis; LS, long single cones; MSA, multiple sequence alignment; NCBP, neuronal Ca$^{2+}$-binding protein; PAGE, polyacrylamide gel electrophoresis; PB, phosphate buffer; PBS, phosphate-buffered saline; PBST, phosphate-buffered saline with 0.1% Triton X-100; TBST, Tris-buffered saline with 0.1% Tween 20; PCR, polymerase chain reaction; ROS, rod outer segment; SS, short single cones.

## References

Ames, J.B., Dizhoor, A.M., Ikura, M., Palczewski, K. & Stryer, L. (1999) Three-dimensional structure of guanylyl cyclase activating protein-2, a calcium-sensitive modulator of photoreceptor guanylyl cyclases. *J. Biol. Chem.*, **274**, 19329–19337.

Applebury, M.L., Antoch, M.P., Baxter, L.C., Chun, L.L., Falk, J.D., Farhangfar, F., Kage, K., Krzystolik, M.G., Lyass, L.A. & Robbins, J.T. (2000) The murine cone photoreceptor: a single cone type expresses both S and M opsins with retinal spatial patterning. *Neuron*, **27**, 513–523.

Barthel, L.K. & Raymond, P.A. (2000) *In situ* hybridization studies of retinal neurons. *Meth. Enzymol.*, **316**, 579–590.

Baylor, D.A. (1987) Photoreceptor signals and vision. *Invest. Ophthalmol. Vis. Sci.*, **28**, 34–49.

Carter-Dawson, L.D. & LaVail, M.M. (1979) Rods and cones in the mouse retina II. Autoradiographic analysis of cell degeneration using tritiated thymidine. *J. Comp. Neurol.*, **188**, 263–272.

Cuenca, N., Lopez, S., Howes, K. & Kolb, H. (1998) The localization of guanylyl cyclase-activating proteins in the mammalian retina. *Invest. Ophthalmol. Vis. Sci.*, **39**, 1243–1250.

Dizhoor, A.M., Boikov, S.G. & Olshevskaya, E. (1998) Constitutive activation of photoreceptor guanylate cyclase by Y99C mutant of GCAP-1. *J. Biol. Chem.*, **273**, 17311–17314.

Dizhoor, A.M., Lowe, D.G., Olshevskaya, E.V., Laura, R.P. & Hurley, J.B. (1994) The human photoreceptor membrane guanylyl cyclase, RetGC, is present in outer segments and is regulated by calcium and a soluble activator. *Neuron*, **12**, 1345–1352.

Dizhoor, A.M., Olshevskaya, E.V., Henzel, W.J., Wong, S.C., Stults, J.T., Ankoudinova, I. & Hurley, J.B. (1995) Cloning, sequencing, and expression of a 24-kDa Ca$^{2+}$-binding protein activating photoreceptor guanylyl cyclase. *J. Biol. Chem.*, **270**, 25200–25206.

Dowling, J.E. (1978) How the retina 'sees.'. *Invest. Ophthalmol. Vis. Sci.*, **17**, 832–834.

Gorczyca, W.A., Gray-Keller, M.P., Detwiler, P.B. & Palczewski, K. (1994) Purification and physiological evaluation of a guanylate cyclase activating protein from retinal rods. *Proc. Natl. Acad. Sci. USA*, **91**, 4014–4018.

Gorczyca, W.A., Polans, A.S., Surgucheva, I., Subbaraya, I., Baehr, W. & Palczewski, K. (1995) Guanylyl cyclase activating protein: a calcium-sensitive regulator of phototransduction. *J. Biol. Chem.*, **270**, 22029–22036.

Goto, K., Miki, N. & Kondo, H. (1989) An immunohistochemical study of pinealocytes of chicks and some other lower vertebrates by means of visinin (retinal cone-specific protein) - immunoreactivity. *Arch. Histol. Cytol.*, **52**, 451–458.

Gregory-Evans, K., Kelsell, R.E., Gregory-Evans, C.Y., Downes, S.M., Fitzke, F.W., Holder, G.E., Simunovic, M., Mollon, J.D., Taylor, R., Hunt, D.M., Bird, A.C. & Moore, A.T. (2000) Autosomal dominant cone-rod retinal dystrophy (CORD6) from heterozygous mutation of GUCY2D, which encodes retinal guanylate cyclase. *Ophthalmology*, **107**, 55–61.

Haeseleer, F., Sokal, I., Li, N., Pettenati, M., Rao, N., Bronson, D., Wechter, R., Baehr, W. & Palczewski, K. (1999) Molecular characterization of a third member of the guanylyl cyclase- activating protein subfamily. *J. Biol. Chem.*, **274**, 6526–6535.

Hisatomi, O., Honkawa, H., Imanishi, Y., Satoh, T. & Tokunaga, F. (1999) Three kinds of guanylate cyclase expressed in medaka photoreceptor cells in both retina and pineal organ. *Biochem. Biophys. Res. Commun.*, **255**, 216–220.

Howes, K., Bronson, J.D., Dang, Y.L., Li, N., Zhang, K., Ruiz, C., Helekar, B., Lee, M., Subbaraya, I., Kolb, H., Chen, J. & Baehr, W. (1998) Gene array and expression of mouse retina guanylate cyclase activating proteins 1 and 2. *Invest. Ophthalmol. Vis. Sci.*, **39**, 867–875.

Kachi, S., Nishizawa, Y., Olshevskaya, E., Yamazaki, A., Miyake, Y., Wakabayashi, T., Dizhoor, A. & Usukura, J. (1999) Detailed Localization of Photoreceptor Guanylate Cyclase Activating Protein-1 and -2 in Mammalian Retinas using Light and Electron Microscopy. *Exp. Eye Res.*, **68**, 465–473.

Kawamura, S., Kuwata, O., Yamada, M., Matsuda, S., Hisatomi, O. & Tokunaga, F. (1996) Photoreceptor protein s26, a cone homologue of S-modulin in frog retina. *J. Biol. Chem.*, **271**, 21359–21364.

Kelsell, R.E., Gregory-Evans, K., Payne, A.M., Perrault, I., Kaplan, J., Yang, R.-B., Garbers, D.L., Bird, A.C., Moore, A.T. & Hunt, D.F. (1998) Mutations in the retinal guanylate cyclase (RETGC-1) gene in dominant con-rod dystrophy. *Hum. Mol. Genet.*, **7**, 1179–1184.

Kimura, M. (1991) The neutral theory of molecular evolution – A review of recent evidence. *Jpn. J. Genet.*, **66**, 367–386.

Kusakabe, T. & Suzuki, N. (2001) A *cis*-regulatory element essential for

photoreceptor cell-specific expression of a medaka retinal guanylyl cyclase gene. *Dev. Genes Evol.*, **211**, 145–149.

Laemmli U.K. (1970) Cleavage of structural proteins during the assembly of the head of bacteriophage T4. *Nature*, **227**, 680–685.

Li, N., Fariss, R.N., Zhang, K., Otto-Bruc, A., Haeseleer, F., Bronson, J.D., Qin, N., Yamazaki, A., Subbaraya, I., Milam, A.H., Palczewski, K. & Baehr, W. (1998) Guanylate cyclase inhibitory protein is a frog retinal Ca$^{2+}$ binding protein related to mammalian guanylate cyclase activating proteins. *Eur. J. Biochem.*, **252**, 591–599.

Li, N., Sokal, I., Bronson, J.D., Palczewski, K. & Baehr, W. (2001) Identification and functional regions of guanylate cyclase-activating protein 1 (GCAP1) using GCAP1/GCIP chimeras. *Biol. Chem.*, **382**, 1179–1188.

Lichtarge, O., Bourne, H.R. & Cohen, F.E. (1996) Evolutionarily conserved G·$\alpha\beta\gamma$ binding surfaces support a model of the G protein-receptor complex. *Proc. Natl. Acad. Sci. USA*, **93**, 7507–7511.

Liu, X., Seno, K., Nishizawa, Y., Hayashi, F., Yamazaki, A., Matsumoto, H., Wakabayashi, T. & Usukura, J. (1994) Ultrastructural localization of retinal guanylate cyclase in human and monkey retinas. *Exp. Eye Res.*, **59**, 761–768.

Lowe, D.G., Dizhoor, A.M., Liu, K., Gu, Q., Spencer, M., Laura, R., Lu, L. & Hurley, J.B. (1995) Cloning and expression of a second photoreceptor-specific membrane retina guanylyl cyclase (RetGC), RetGC-2. *Proc. Natl. Acad. Sci. USA*, **92**, 5535–5539.

Mendez, A., Burns, M.E., Sokal, I., Dizhoor, A.M., Baehr, W., Palczewski, K., Baylor, D.A. & Chen, J. (2001) Role of guamylate cyclase-activating proteins (GCAPs) in setting the flash sensititvity of rod photoreceptors. *Proc. Natl. Acad. Sci. USA*, **98**, 9948–9953.

Mighell, A.J., Smith, N.R., Robinson, P.A. & Markham, A.F. (2000) Vertebrate pseudogenes. *FEBS Lett.*, **468**, 109–114.

Olshevskaya, E.V., Boikov, S., Ermilov, A., Krylov, D., Hurley, J.B. & Dizhoor, A.M. (1999) Mapping Functional Domains of the Guanylate Cyclase Regulator Protein, GCAP-2. *J. Biol. Chem.*, **274**, 10823–10832.

Otto-Bruc, A., Fariss, R.N., Haeseleer, F., Huang, J., Buczylko, J., Surgucheva, I., Baehr, W., Milam, A.H. & Palczewski, K. (1997) Localization of guanylate cyclase activating protein 2 in mammalian retinas. *Proc. Natl. Acad. Sci. USA*, **94**, 4727–4732.

Palczewski, K., Subbaraya, I., Gorczyca, W.A., Helekar, B.S., Ruiz, C.C., Ohguro, H., Huang, J., Zhao, X., Crabb, J.W., Johnson, R.S., Walsh, K.A., Gray-Keller, M.P., Detwiler, P.B. & Baehr, W. (1994) Molecular cloning and characterization of retinal photoreceptor guanylyl cyclase activating protein (GCAP). *Neuron*, **13**, 395–404.

Payne, A.M., Downes, S.M., Bessant, D.A., Taylor, R., Holder, G.E., Warren, M.J., Bird, A.C. & Bhattacharya, S.S. (1998) A mutation in guanylate cyclase activator 1A (GUCA1A) in an autosomal dominant cone dystrophy pedigree mapping to a new locus on chromosome 6p21.1. *Hum. Mol. Genet.*, **7**, 273–277.

Perrault, I., Rozet, J.-M., Calvas, P., Gerber, S., Camuzat, A., Dollfus, H., Chatelin, S., Souied, E., Ghazi, I., Leowski, C., Bonnermaison, M., Le Paslier, D., Frezal, J., Dufier, J.-L., Pittler, S.J., Munnich, A. & Kaplan, J. (1996) Retinal-specific guanylate cyclase gene mutations in Leber's congenital amaurosis. *Nature Genet.*, **14**, 461–464.

Perrault, I., Rozet, J.M., Gerber, S., Ghazi, I., Ducroq, D., Souied, E., Leowski, C., Bonnemaison, M., Dufier, J.L., Munnich, A. & Kaplan, J. (2000) Spectrum of retGC1 mutations in Leber's congenital amaurosis. *Eur. J. Hum. Genet.*, **8**, 578–582.

Polans, A., Baehr, W. & Palczewski, K. (1996) Turned on by Ca$^{2+}$! The physiology and pathology of Ca$^{2+}$-binding proteins in the retina. *Trends Neurosci.*, **19**, 547–554.

Polans, A.S., Burton, M.D., Haley, T.L., Crabb, J.W. & Palczewski, K. (1993) Recoverin, but not visinin, is an autoantigen in the human retina identified with a cancer-associated retinopathy. *Invest. Ophthalmol. Vis. Sci.*, **34**, 81–90.

Raymond, P.A., Barthel, L.K., Rounsifer, M.E., Sullivan, S.A. & Knight, J.K. (1993) Expression of rod and cone visual pigments in goldfish and zebrafish: a rhodopsin-like gene is expressed in cones. *Neuron*, **10**, 1161–1174.

Rodieck, R.W. (1998) *The First Steps in Seeing*. Sinauer Associates, Sunderland, MA.

Rosen, B. & Beddington, R. (1994) Detection of mRNA in whole mounts of mouse embryos using digoxigenin riboprobes. *Meth. Mol. Biol.*, **28**, 201–208.

Schoenmakers, T.J., Visser, G.J., Flik, G. & Theuvenet, A.P. (1992) CHELATOR: an improved method for computing metal ion concentrations in physiological solutions. *Biotechniques*, **12**, 870–879.

Schrem, A., Lange, C., Beyermann, M. & Koch, K.W. (1999) Identification of

a domain in guanylyl cyclase-activating protein 1 that interacts with a complex of guanylyl cyclase and tubulin in photoreceptors. *J. Biol. Chem.*, **274**, 6244–6249.

Seimiya, M., Kusakabe, T. & Suzuki, N. (1997) Primary structure and differential gene expression of three membrane forms of guanylyl cyclase found in the eye of the teleost Oryzias latipes. *J. Biol. Chem.*, **272**, 23407–23417.

Semple-Rowland, S.L., Lee, N.R., Van-Hooser, J.P., Palczewski, K. & Baehr, W. (1998) A null mutation in the photoreceptor guanylate cyclase gene causes the retinal degeneration chicken phenotype. *Proc. Natl. Acad. Sci. USA*, **95**, 1271–1276.

Shyjan, A.W., de Sauvage, F.J., Gillett, N.A., Goeddel, D.V. & Lowe, D.G. (1992) Molecular cloning of a retina-specific membrane guanylyl cyclase. *Neuron*, **9**, 727–737.

Sokal, I., Li, N., Klug, C.S., Filipek, S., Hubbell, W.L., Baehr, W. & Palczewski, K. (2001) Calcium-sensitive regions of GCAP1 as observed by chemical modifications, fluorescence and EPR spectroscopies. *J. Biol. Chem.*, **276**, 43361–43373.

Sokal, I., Li, N., Surgucheva, I., Warren, M.J., Payne, A.M., Bhattacharya, S.S., Baehr, W. & Palczewski, K. (1998) GCAP1 (Y99C) mutant is constitutively active in autosomal dominant cone dystrophy. *Mol. Cell*, **2**, 129–133.

Sowa, M.E., He, W., Slep, K.C., Kercher, M.A., Lichtarge, O. & Wensel, T.G. (2001) Prediction and confirmation of a site critical for effector regulation of RGS domain activity. *Nat. Struct. Biol.*, **8**, 234–237.

Sowa, M.E., He, W., Wensel, T.G. & Lichtarge, O. (2000) A regulator of G protein signalling interaction surface linked to effector specificity. *Proc. Natl. Acad. Sci. USA*, **97**, 1483–1488.

Subbaraya, I., Ruiz, C.C., Helekar, B.S., Zhao, X., Gorczyca, W.A., Pettenati, M.J., Rao, P.N., Palczewski, K. & Baehr, W. (1994) Molecular characterization of human and mouse photoreceptor guanylate cyclase activating protein (GCAP) and chromosomal localization of the human gene. *J. Biol. Chem.*, **269**, 31080–31089.

Surguchov, A., Ruiz, C.C., Rao, P.N., Palczewski, K. & Baehr, W. (1996) Cloning, expression, and chromosomal localization of the human and mouse GCAP2 gene. *Invest. Ophthalmol. Vis. Sci.*, **37**, 335.

Tucker, C.L., Woodcock, S.C., Kelsell, R.E., Ramamurthy, V., Hunt, D.M. & Hurley, J.B. (1999) Biochemical analysis of a dimerization domain mutation in RetGC-1 associated with dominant cone-rod dystrophy. *Proc. Natl. Acad. Sci. USA*, **96**, 9039–9044.

Van Ghelue, M., Eriksen, H.L., Ponjavic, V., Fagerheim, T., Andreasson, S., Forsman-Semb, K., Sandgren, O., Holmgren, G. & Tranebjaerg, L. (2000) Autosomal dominant cone-rod dystrophy due to a missense mutation (R838C) in the guanylate cyclase 2D gene (GUCY2D) with preserved rod function in one branch of the family. *Ophthalmic Genet*, **21**, 197–209.

Yang, R.B. & Garbers, D.L. (1997) Two eye guanylyl cyclases are expressed in the same photoreceptor cells and form homomers in preference to heteromers. *J. Biol. Chem.*, **272**, 13738–13742.

Yang, R.B., Robinson, S.W., Xiong, W.H., Yau, K.W., Birch, D.G. & Garbers, D.L. (1999) Disruption of a retinal guanylyl cyclase gene leads to cone-specific dystrophy and paradoxical rod behavior. *J. Neurosci.*, **19**, 5889–5897.